

Performance of open-path lasers and FTIR spectroscopic systems in agriculture emissions research

Mei Bai¹, Zoe Loh², David W. T. Griffith³, Debra Turner¹, Richard Eckard¹, Robert Edis¹, Owen T. Denmead⁴, Glenn W. Bryant³, Clare Paton-Walsh³, Matthew Tonini³, Sean M. McGinn⁵, Deli Chen¹

¹Faculty of Veterinary and Agricultural Sciences, The University of Melbourne, Parkville, VIC 3010, Australia

²CSIRO Oceans & Atmosphere, PMB 1, Aspendale, VIC 3195, Australia

³School of Chemistry & Centre for Atmospheric Chemistry, University of Wollongong Wollongong, NSW 2522, Australia

⁴Deceased, CSIRO Agriculture and Food, GPO Box 1666, Canberra, ACT 2601, Australia

⁵Agriculture and Agri-Food Canada, Lethbridge, Alberta, Canada

Correspondence to Mei Bai (mei.bai@unimelb.edu.au)

Abstract. The accumulation of gases into our atmosphere is a growing global concern that requires considerable quantification of the emission rates and mitigate the accumulation of gases in the atmosphere, especially the greenhouse gases (GHG). In agriculture there are many sources of GHG that require attention in order to develop practical mitigation strategies. Measuring these GHG sources often rely on highly technical instrumentation originally designed for applications outside of the emissions research in agriculture. Although the open-path laser (OPL) and open-path Fourier transform infrared (OP-FTIR) spectroscopic techniques are used in agricultural research currently, insight into their contributing error to emissions research has not been the focus of these studies. The objective of this study was to assess the applicability and performance (accuracy and precision) of OPL and OP-FTIR spectroscopic techniques for measuring gas mole fraction from agricultural sources. We measured the mole fractions of trace gases methane (CH₄), nitrous oxide (N₂O), and ammonia (NH₃), downwind of point and area sources with known release rate. The mole fractions measured by OP-FTIR and OPL were also input into models of atmospheric dispersion (WindTrax) allowing the calculation of fluxes. Trace gas release recoveries with Windtrax were examined by comparing the ratio of estimated and known fluxes. The OP-FTIR provided the best performance regarding stability of drift in stable conditions. The CH₄ OPL accurately detected the low background (free-air) level of CH₄; however, the NH₃ OPL was unable to detect the background values < 10 ppbv. The dispersion modelling using WindTrax coupled with open path measurements can be a useful tool to calculate trace gas fluxes from the well-defined source area.

Keywords: spectroscopy, open path, trace gas, mole fraction, WindTrax modelling

1 Introduction

Globally, agriculture contributes approximately 10–12% of anthropogenic greenhouse gases (GHG) entering the atmosphere in 2010 (Smith et al., 2014). The majority of these emissions come from the livestock sector, which includes methane (CH₄) from enteric fermentation in ruminants, direct nitrous oxide (N₂O) from animal excreta through the nitrification and denitrification processes, and indirect greenhouse effects due to N leaching, runoff, and atmospheric deposition of ammonia (NH₃) vitalization from manure by forming N₂O emissions (called indirect

36 N₂O emissions). Globally, the indirect N₂O emissions account for one third of the total N₂O emissions from
37 agricultural sector (de Klein et al., 2006).

38
39 Direct field measurements of agricultural GHG emissions are difficult due to its high spatial and temporal variation,
40 diverse source emissions, and lack of appropriate measurement techniques. Consequently, the Intergovernmental
41 Panel on Climate Change (IPCC, 2006) and Australia's National Greenhouse Gas Inventory Committee (NIR,
42 2015) use national emission rates that have been based primarily on extrapolations of laboratory and enclosure
43 measurements. Such extreme extrapolations are subject to greater uncertainty than would be the situation if farm-
44 scaled values were used. Meeting international obligations on GHG reporting should ultimately require non-
45 intrusive emission measurements at an appropriate regional scale. Moreover, development, implementation and
46 adaptation of mitigation strategies rely on well-developed measurement methodologies.

47
48 Although considerable effort is being made to document GHG emissions from land-management practices, the
49 measurement techniques employed in that endeavour are not ideal. Surface chamber method is typically used to
50 measure gas fluxes from the soil surface, but substantial numbers of surface chambers are required to reduce the
51 temporal and spatial variations in gas emissions from large scale source (McGinn, 2006). Mass balance techniques
52 measured emissions from a source area are based on the total influx and efflux of each gas carried into and out of a
53 control volume (Denmead, 1995). Original applications of this method required the targeted source area to be bounded
54 by a "fence" of sampling pipes that extended to the upper limit of the gas plume generated from the source. Influxes
55 and effluxes were calculated by integrating the horizontal fluxes (the product of wind speeds and gas mole fractions)
56 across the boundaries (Denmead et al., 1998). The plume generated from an area source is expected to extend up to a
57 height of at least one-tenth of the upwind fetch. Two technological developments together offer a considerable
58 simplification and flexibility of this basic mass balance technique. The advent of open-path (OP) gas analysers has
59 enabled the measurement of average mole fractions over long path lengths, removing the need for sampling tubes,
60 pumps and multiplexing to a closed-path analyser. In addition, mathematical models of atmospheric dispersion allow
61 fluxes to be inferred from mole fraction measurements and boundary layer wind statistics. Studies of using these
62 combined OP and dispersion techniques have been reported extensively, such as dairy farms (Bjorneberg et al., 2009;
63 Harper et al., 2009; VanderZaag et al., 2014), grazing cattle (Laubach et al., 2016; Tomkins et al., 2011), cattle feedlots
64 (Bai et al., 2015; Loh et al., 2008; McGinn and Flesch, 2018), boiler production (Harper et al., 2010), storage lagoon
65 (Bühler et al., 2020; McGinn et al., 2008), animal waste treatment (Bai et al., 2020; Flesch et al., 2011; Flesch et al.,
66 2012), bush fire (Paton-Walsh et al., 2014), geosequestration from industries (Feitz et al., 2018; Loh et al., 2009), and
67 urban vehicle emissions (Phillips et al., 2019). Although these combined OP and dispersion techniques have
68 increasingly gained researchers' attentions as a useful tool in measuring gas emissions from large scale field, such as
69 insight into the OP sensors contributing error to emissions research has not been the focus of these studies.

70
71 The purpose of our study is to evaluate these two techniques for measuring GHG emissions from agricultural lands.
72 Two OP spectroscopic techniques are used to determine line-averaged mole fractions in the field measurements. The

73 underlying principles of the method and the accuracy and precision of the broad band OP-Fourier transform infrared
74 spectrometer (FTIR) and single band OP-laser (OPL) spectrometer are tested at experimental sites using releases of
75 gases at known rates from a point and area sources. We measured the mole fractions (in air) of CH₄, NH₃ and N₂O
76 with two spectroscopic techniques when gas was released at a known rate. The mole fractions measured by OP-FTIR
77 and OPL were also input into models of atmospheric dispersion (WindTrax) allowing the calculation of fluxes. Trace
78 gas release recoveries with Windtrax were examined by comparing the ratio of calculated and known fluxes. This
79 study would be the first paper of solely comparing the performance between OP mole fraction sensors and provide
80 the information as reference for measurement techniques in large-scale gas emission research.

81 **2 Materials and Methods**

82 **2.1 Experimental design**

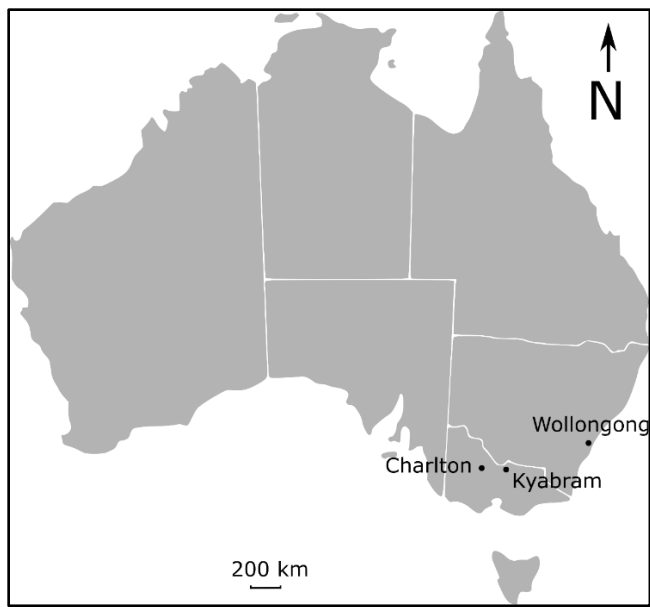
83 The field measurement campaigns were conducted at three sites (Fig. 1):

84 *Kyabram, Victoria DPI Irrigated dairy research farm* (36.34°S, 145.06°E, elevation 104 m). This is a well-established
85 research site ideal for micrometeorological measurements, with flat terrain and an existing suite of instrumentation.
86 Measurements were set up in two adjacent bays near the existing micrometeorological site. The principal disadvantage
87 of this site was the considerable variation in background trace gas mole fractions (particularly CH₄), due to the high
88 cattle population in the region.

89 *University of Wollongong* (34.41°S, 150.88°E, elevation 26 m). The No.3 sports oval at the University of Wollongong
90 is a flat, grassed area approximately 200-250 m in extent. It is surrounded by trees and not a suitable site for
91 micrometeorological measurements but was well suited to trial release measurements and early OP-FTIR field tests.

92 *Commercial beef cattle feedlot, Victoria* (225 km northwest of Melbourne, Australia). This site was used for
93 comparisons of sensors side-by-side experiments. The farm is flat and well suited to micrometeorological
94 measurements of CH₄ emissions from cattle pens.

95



96
97 **Figure 1: Three experimental sites at Wollongong sports field, Kyabram research centre, and a feedlot at Charlton.**

98 The trace gas release measurements including point and area sources were conducted at Kyabram and Wollongong,
99 assuming that all trace gases (CH₄, NH₃, and N₂O) disperse equally from source to open path (OP). Two OP sensors
100 were trialled – a broad band FTIR spectrometer (OP-FTIR) and a single wavelength laser-based instrument (OPL).
101 Besides the gas release measurements, two OP-FTIR sensors were also conducted a side-by-side comparison of
102 measuring gas mole fractions from cattle pens at a commercial beef cattle feedlot. A summary of these trials is shown
103 in Table 1.

104
105 **Table 1. Summary of field measurements at Kyabram, Wollongong, and the Victorian feedlot. Target gases,**
106 **instrumentations used for the studies, and study durations are also shown.**

Location	Trial Date	Experiment	Pathlength/m	Height/m	Target Gases	OP sensor ^δ
Kyabram	25-29 July 2005	Gas releases, point sources	137/125	0.5	CH ₄ , N ₂ O, NH ₃	OP-FTIR [§]
	1-4 Aug. 2005	Gas releases, area sources, Side-by-side comparison	137/125	Ground	CH ₄ , NH ₃	OP-FTIR [§] , OPL
	21 Mar. 2006	Herd of cattle Side-by-side comparison	227	1,7*	CH ₄ , NH ₃	OP-FTIR, OPL (CH ₄)

Wollongong	14-18 May 2005	Gas releases, point sources, Side-by-side comparison	87.5/150	1.28	CH ₄ , N ₂ O, NH ₃	OP-FTIR [§] ,
	15-16 Mar. 2006	Gas releases, point sources, Side-by-side comparison	148	0.5/1.28	CH ₄ , NH ₃	OP-FTIR [§] , OPL
Commercial feedlot	28 Feb.- 5 Mar. 2008	Side-by-side comparison	100	1.7 [*]	CH ₄ , N ₂ O,	OP-FTIR [§] , OP-FTIR [‡]

107 [§] (Bomem)

108 [‡] (Bruker)

109 ^{*} cattle were the main CH₄ source, the average of cattle height was 1.7 m.

110 ^δ the path length for all OP sensors was 1.5 m above the ground.

111

112 **Table 2. Gas release times, rates, and source types for controlled release experiments at Kyabram DPI (July-August 2005).**
113 Mass flows measured in standard litres per minute (21°C and 1 atm) have been converted to mg s⁻¹.

Date	Time	Source	OP-FTIR Path	OPL Path	Release rates (mg s ⁻¹)		
					CH ₄	NH ₃	N ₂ O
27/07/2005	10:47 - 12:52	1	1	-	55.37	58.80	151.95
	12:52 - 14:17	1	1	-	99.67	105.84	151.95
	15:13 - 16:18	2	1	-	99.67	105.84	151.95
28/07/2005	17:47 - 08:23	2	1	-	27.69	29.40	75.97
	10:44 - 14:41	2	1	-	55.37	58.80	151.95
	14:41 - 16:42	2	1	-	99.67	105.84	151.95
29/07/2005	17:29 - 10:52	1	1	-	27.69	29.40	75.97
	10:52 - 11:33	1	1	-	11.07	11.76	30.39
	11:33 - 12:05	1	1	-	5.54	5.88	15.19
1/08/2005	12:43 - 13:51	1	1	-	27.69	29.40	75.97
	13:51 - 14:25	1	1	-	55.37	58.80	151.95
	14:25 - 15:00	1	1	-	99.67	105.84	273.51
	15:00 - 15:30	1	1	-	55.37	58.80	151.95
	15:30 - 16:00	1	1	-	11.07	11.76	30.39
	16:00 - 16:30	1	1	-	2.77	2.94	7.60
1/08/2005	15:17 - 15:45	1	1	-	55.37	105.84	0.00
	15:45 - 16:58	1	1	-	55.37	105.84	151.95

	17:18 - 18:16	1	1	-	55.37	0.00	303.90
	18:16 - 09:00	3	1	-	55.37	58.80	151.95
2/08/2005	12:46 - 16:17	3	2	2 [‡]	55.37	58.80	151.95
	17:08 - 18:19	4	2	2 [‡]	5.54	5.88	15.19
	18:19 - 08:55	4	2	2 [‡]	5.54	0.00	15.19
3/08/2005	08:55 - 09:15	4	2	2 [‡]	5.54	5.88	15.19
	09:15 - 09:33	4	2	2 [‡]	0.00	2.35	0.00
	09:33 - 10:26	4	2	2 [‡]	55.37	58.80	151.95

114 [‡]OPL NH₃ sensor only. Laser path was located 3 m north of path 2.

115 [‡]OPL NH₃ and OPL CH₄ sensor. OPL CH₄ path was located 3 m south of path 2.

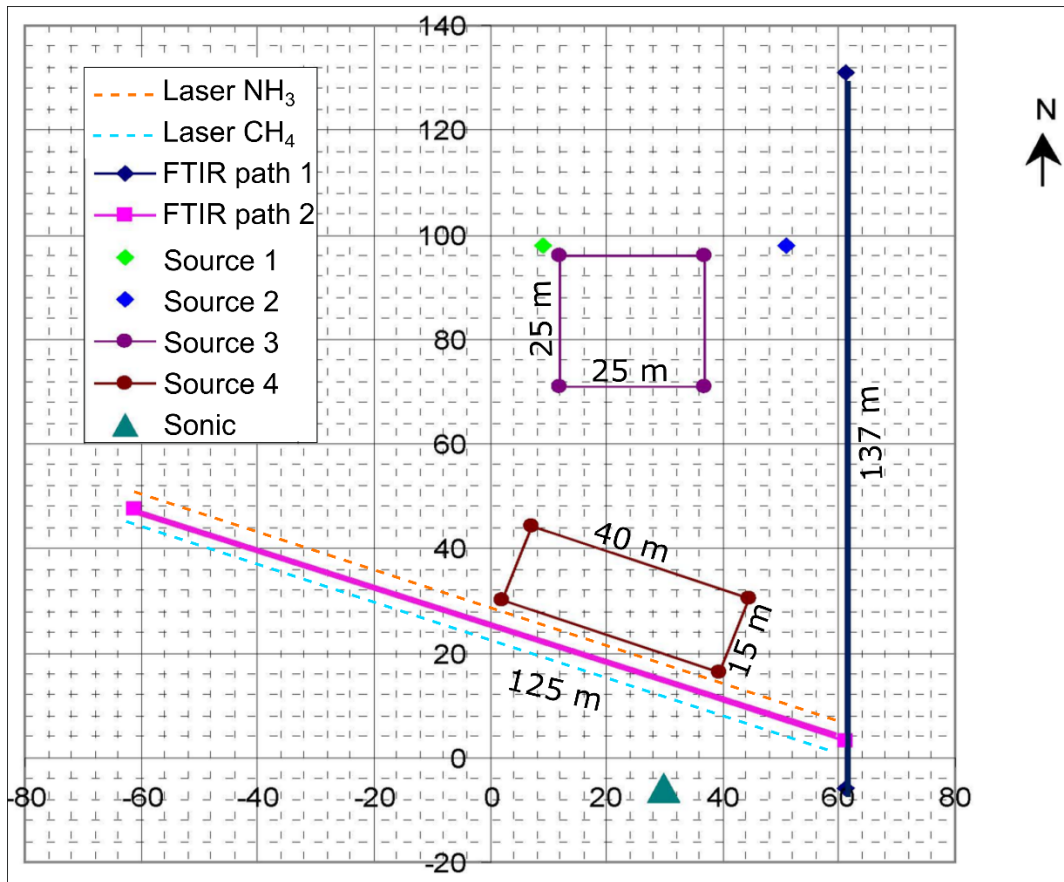
116 2.2 Gas release experiments

117 The underlying principles of the method and the accuracy and precision of the OP-FTIR and laser spectrometers were
 118 tested at Kyabram and Wollongong using releases of CH₄, N₂O, and NH₃ at known rates from a common point or area
 119 source.

120

121 We first conducted the gas release measurements at Kyabram during a period of suitable conditions of steady wind
 122 and near neutral stability, and there were no other strong sources of CH₄, N₂O, and NH₃ nearby. Gas release points
 123 (sources 1 and 2) were located to the west of the OP-FTIR path 1, which ran N-S along the fence line (Fig. 2). Area
 124 sources (sources 3 and 4) were located to the north of the OP-FTIR path 2, which ran NW-SE direction (Fig. 2). The
 125 OPL sensors (NH₃ and CH₄) were set up on the north and south parallel to OP-FTIR path 2, respectively (Fig.2). The
 126 path height for all OP sensors was 1.7 m above ground level and the measurement path lengths were 137 and 125 m
 127 (two-way path) for path 1 and 2, respectively. The gas release heights varied from ground level (area sources) to 0.5
 128 m above ground level (point sources). The layout of sources and open path geometries at Kyabram are summarised in
 129 Figure 2. A summary of the gas release times, source types and OP sensor measurement paths used at Kyabram is
 130 shown in Table 2.

131



132

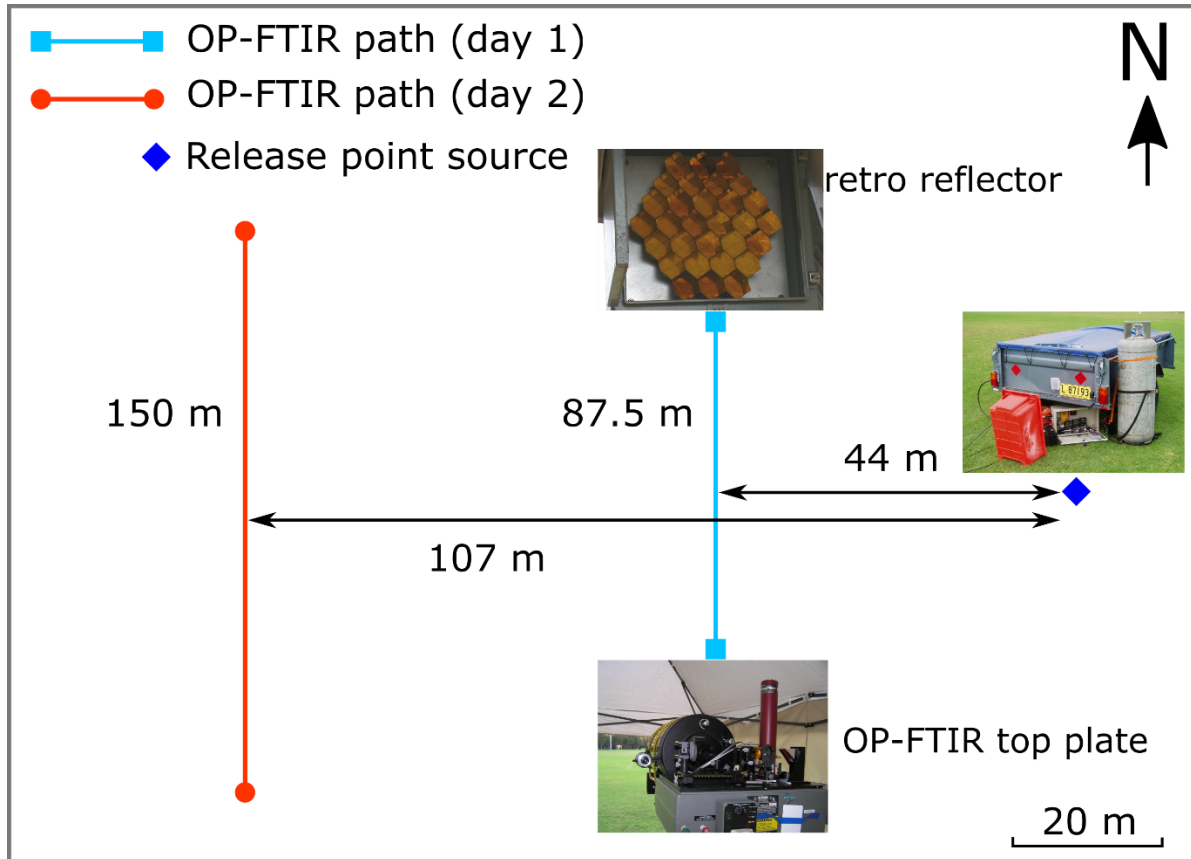
133 **Figure 2: Point and area gas release sources and OP sensors path geometries (distances in m) at Kyabram July-August**
 134 **2005. Point source 1 is in green and 2 is in blue. Area source 3 is 25 × 25 m, and area source 4 is 40 × 15 m. The OP-FTIR**
 135 **measurement path lengths 1 and 2 were 137 and 125 m (two-way path), respectively. OPL NH₃ and CH₄ sensor were parallel**
 136 **to OP-FTIR path 2 (dashed yellow and blue lines respectively). Sonic anemometer was located to the south of the site (dark**
 137 **green triangle).**

138 During the point source release trials, one OP-FTIR was set up on path 1. CH₄ and NH₃ were released at 9 std L min⁻¹
 139 (SLPM) and N₂O was released at 5 SLPM, from a single release point, over a three-day study (1-3 August 2005)
 140 (Fig. 2). These were point sources, not distributed as cattle or soil would be. The aim was to show that the known
 141 fluxes can be retrieved from the measurements, for all three gases. In this case it is permissible to have higher emissions
 142 than those typical in the field to minimize uncertainty due to background variability.

143

144 The first trial of area source release measurements was undertaken on the evening of 1 August 2005 using the 25 × 25
 145 m area source (source 3) and path 1. Unfortunately, wind conditions were E winds dominated that very little of the
 146 released plume crossed the measurement path. Subsequently, a period in the middle of the day with source 3 and path
 147 2 was employed using the lasers (NH₃ only) and one OP-FTIR. The OP-FTIR was set up on the path 2 and laser NH₃
 148 sensors were run parallel 3 m north of the OP-FTIR path. Thereafter, the area source 4 (40 × 15 m) and path 2 were
 149 used coupled with the lasers (NH₃ and CH₄) and the OP-FTIR. Two OPL_CH₄ lasers were located 8 m downwind
 150 from the area source, two OPL_NH₃ sensors were run parallel 2 m downwind of area source, and OP-FTIR at 5 m
 151 downwind of the source at the same time (Fig. 2). The path height for all OP sensors was 1.7 m and the measurement

152 path lengths were 137 and 125 m for path 1 and 2, respectively. The different path length was determined depending
 153 on the factors of wind conditions (direction and wind speed) and the distance between the path length and source area.
 154 Given the constant wind direction, the longer pathlength was needed when the measurement path was further away
 155 from the source so that the gas plume could pass by most of the OP measurement path.
 156

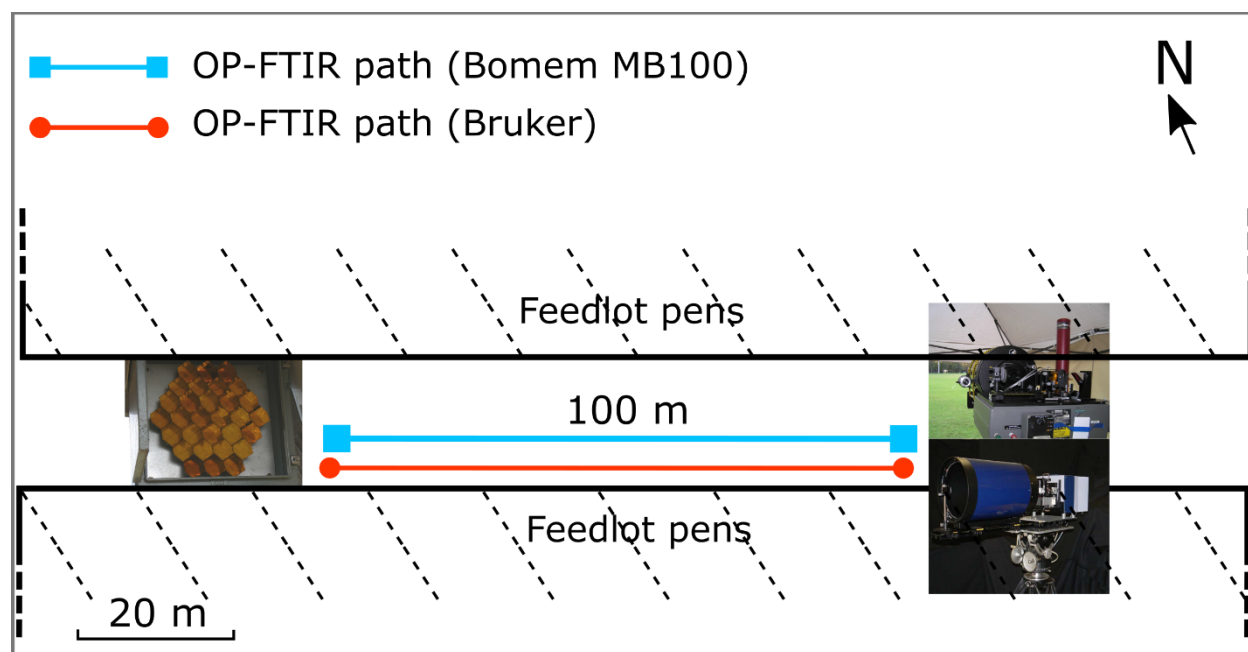


157
 158 **Figure 3: Point gas release sources and OP-FTIR path geometries (distances in m) at Wollongong August 2005. The OP-**
 159 **FTIR measurement path lengths at day 1 and 2 were 87.5 and 150 m (two-way path), respectively. Three ¼” tubes coming**
 160 **from three tanks (CH₄ (natural gas), NH₃ and N₂O) bundled together on a stake at the release height 1.28 m above ground**
 161 **level.**

162 The OP-FTIR was also examined at Wollongong sports field during a release trial from for two days (Fig. 3). NH₃,
 163 CH₄, and N₂O were released at the point source (1.28 m above ground level). The path length of OP-FTIR and its
 164 distance from the source was initially 87.5 (two-way path) and 44 m, respectively, the OP-FTIR was then moved
 165 further away from the source, 107 m from the source with a longer measurement path of 150 m (two-way path).
 166

167 Furthermore, to check the long-term performance of precision and accuracy of the instruments, we conducted side-
 168 by-side measurements to evaluate sensor differences at Wollongong and a commercial feedlot in northwest of Victoria.
 169 During the intercomparison of OPL and OP-FTIR at Wollongong, the OPL sensors (two for CH₄ and two for NH₃)
 170 and the Bomem OP-FTIR recorded mole fractions over a path length of 148 m (two-way path) before and after the
 171 gases were released. At the commercial feedlot (Fig. 4), two OP-FTIR spectrometers were run side-by-side. Mole

172 fractions of CH₄, N₂O, and NH₃ were simultaneously measured for 6 days with the path length of 100 m (two-way
 173 path), and measurement height of 1.5 m above the ground. Flasks (600 millilitre, mL) were evacuated prior to gas
 174 sampling. Each sample day during stable boundary layer conditions (Monin-Obukov length L, $L \cong 0-10$ m), air
 175 samples were collected simultaneously at three points (0, 50, 100 m from the spectrometer) along the measurement
 176 path. Total 14 samples over a 5-day period were collected. The air samples were analysed using a closed-path FTIR
 177 at the off-site laboratory at University of Wollongong, which has been calibrated to the standard gases CH₄ and N₂O
 178 (Griffith et al., 2012). The concurrent mole fractions of CH₄ and N₂O, measured by two FTIR were compared to that
 179 of air samples.
 180



181
 182 **Figure 4: Two OP-FTIR spectrometers (Bomem MB100 and Bruker) during side-by-side operation in a commercial**
 183 **feedlot in Victoria in February 2008.**

184 **2.3 Gas release system**

185 The controlled gas releases were of NH₃ (>99%, BOC refrigeration grade, Australia), CH₄ (compressed natural gas,
 186 89% CH₄, Agility, Australia), and N₂O (>99%, BOC Instrument grade, Australia) supplied from high pressure
 187 cylinders. Each of the gas flows was controlled by a mass flow controller with $\pm 2\%$ full scale repeatability (Smart-
 188 Trak™ series 100, Sierra Instruments Inc., California, USA). Each gas cylinder was connected to the mass flow
 189 controller with 1/4" nylon tubing, the gas outflow from each mass flow controller was released to the atmosphere
 190 through another length of nylon tubing. Each gas flow controller was scaled for the gas measurement using the
 191 manufacturer's data. Controlled gas flow rates were logged every minute using a data logger (DataTaker, Melbourne).
 192 For point-source emissions, the outlets of the three gases were co-located at a release height of 0.5-1.28 m above
 193 ground. For surface area emissions, the flows were fed into a length of drip-irrigation tubing (Miniscape, 8 mm) with
 194 valve holes every 2.5 m and spread over a 25 × 25 m or 40 × 15 m grid at ground level.

195 2.4 Open-path spectrometers

196 2.4.1 Open-path lasers

197 Four open-path lasers (OPL, GasFinder2.0, Boreal Laser Inc, Edmonton, Alberta, Canada) were used. Two units (1012
198 and 1013) measured CH₄, the other two (1015 and 1016) measured NH₃. Each OPL was associated with a remote
199 passive retro reflector that delineated the path. The OPL contains a transceiver that houses the laser diode, drive
200 electronics, detector module and micro-computer subsystems. Collimated light emitted from the transceiver traverses
201 the OP to the retro reflector and back. A portion of the beam passes through an internal reference cell. Trace gas mole
202 fraction in the optical path is determined from the ratio of measured external and reference signals. Sample scans are
203 made at approximately 1 s interval and the data were stored internally as one-minute averages. Transceivers are
204 portable, tripod-mounted, battery operated (12 VDC). The retro reflector is tripod-mounted and composed of an array
205 of six gold-coated 6 cm corner cubes with effective diameters of approximately 20 cm. Alignment of transceiver and
206 retro reflector is straightforward and generally stable for several hours over path lengths up to 500 m. The nominal
207 sensitivity of the laser units is 1 part per million-metre (ppm-m), corresponding to 10 ppb for a 100-m path.

208 2.4.2 Open-path FTIR

209 There were two different OP-FTIR units used in these studies. The first unit consisted of a Bomem MB100-2E OP-
210 FTIR spectrometer (ABB Bomem, Quebec, Canada) and a modified Meade 30.5 cm diameter LX200 Schmidt-
211 Cassegrain telescope that were assembled at the University of Wollongong along with software (Tonini, 2005).
212 Operationally, the transfer optics take the modulated infrared radiation from the FTIR through the telescope to reduce
213 beam divergence to a set of retro reflectors placed at some distance away, collect the returned radiation, and focus the
214 radiation onto a liquid nitrogen cooled MCT detector. A Zener-diode thermometer (type LM335) and a barometer
215 (PTB110, Vaisala, Helsinki, Finland) provide real-time air temperature and pressure data for the analysis of the
216 measured spectra. The spectrometer is operated at 1 cm⁻¹ resolution, and one spectrometer scan takes approximately
217 4 secs (13 scans min⁻¹). For acceptable signal to noise ratios, scans are generally averaged for at least 1 minute.
218 Immediately following each measurement, the spectrum is analysed (see below) and calculated mole fractions are
219 displayed and logged in real time together with ambient pressure and temperature. Operation is continuous and fully
220 automated by the software to control the spectrometer, data logging and spectrum analysis (Paton-Walsh et al., 2014).
221 Under normal operation the detector must be re-filled with liquid nitrogen once per day, and occasional re-alignment
222 of the spectrometer on the tripod may be required depending on the stability of the tripod footings.

223

224 Quantitative analysis to determine trace gas mole fractions from OP-FTIR spectra is based on non-linear least squares
225 fitting of the measured spectra by a computed spectrum based on the HITRAN (high-resolution transmission
226 molecular absorption) database of spectral line parameters (Rothman et al., 2009; Rothman et al., 2005) using a model
227 calculation (Griffith, 1996). The OP-FTIR spectrum is iteratively calculated until a best fit to the measured spectrum
228 is obtained. The mole fraction of absorbing species in the open path is obtained from the best-fit input parameters to
229 the calculated spectrum (Griffith, 1996; Smith et al., 2011). The OP-FTIR spectrometer measures the broadband IR
230 spectrum simultaneously over the range 600-5000 cm⁻¹. The three separate spectral regions (N₂O (2130–2283 cm⁻¹),

231 CH₄ (2920–3020 cm⁻¹), and NH₃ (900–980 cm⁻¹) are extracted from the broadband spectrum and analyzed separately
232 for each target species.

233
234 The second OP-FTIR unit was the Bruker IRCube spectrometer (Matrix-M IRCube, Bruker Optics, Ettlingen,
235 Germany) that was developed based on the same principle of Bomem spectrometer (University of Wollongong)
236 (Paton-Walsh et al., 2014; Phillips et al., 2019). This Bruker OP-FTIR replaced the liquid nitrogen (N₂) system by a
237 Stirling cycle mechanical refrigerator, and a 25.4 cm diameter telescope and a secondary mirror were built to create a
238 25-mm parallel beam to extend the measurement path up to 500 m. The analytical spectral regions are the same as
239 Bomem MB 100. More details of Bruker IRCube spectrometer can be found in Bai (2010). The system parameters
240 from both OP-FTIR are summarized in Table 3. Recently, a custom-made motorised tripod head has been installed to
241 allow the spectrometer to be aimed at multiple paths where the retro-reflectors were separated vertically or horizontally
242 (Bai et al., 2016; Flesch et al., 2016).

243

244 **Table 3. The system parameters between OP-FTIR Bomem MB100 and Bruker IR cube spectrometer.**

	Bomem MB100	Bruker IRCube
Detector	Liquid N ₂ cooled MCT	Stirling cycle refrigerator cooled MCT
Size of telescope	30.5 cm	25.4 cm
SNR ^{§#}	~6000	~9000
Weight	Heavy	Light
Optics dust proof	No	Yes
Motorised aiming system	No	Yes

245 [§] SNR, signal to noise ratio. A transmission spectrum is calculated by taking ratios of two successive spectra and measuring root
246 mean square (rms) noise at a spectral region 2500-2600 cm⁻¹.

247 [#] measured over 100 m path length (two-way path).

248

249 **2.5. Dispersion modelling (WindTrax)**

250 To infer emission source strengths or fluxes from atmospheric mole fraction measurements, we require a means to
251 quantify atmospheric transport and dispersion of the target trace gases between source and measuring point. Our
252 approach is to infer area-averaged surface fluxes (in excess of background) from measured line-average mole fractions
253 by using a backward Lagrangian stochastic (bLs) model as developed by Flesch et al. (2004; 1995). The bLs model is
254 capable of handling sources of arbitrary size and geometry. The model is encoded in the commercially available
255 software package WindTrax (version 1.0, Thunder Beach Scientific) (Crenna et al., 2006). The inputs for WindTrax
256 bLs model include the measured mole fraction, sonic anemometer measurements of wind speed and direction, stability
257 and turbulence as well as other micrometeorological parameters. The WindTrax bLs model simulates the backwards
258 trajectories of molecules sensed in the optical path. The instrument tower (in the source area) provides the information
259 necessary to calculate the trajectories. In this study, 50,000 parcels are released and propagated backward to build up
260 a statistical distribution of trajectories from which source strengths can be calculated. “Touchdowns” are partitioned

261 into those originating in the source area and those from the background. This allows the net flux of particles across
262 the path to be separated into contributions from source and background level.

263
264 Similar to the studies in McGinn et al. (2006), we predicted tracer release rates by measuring downwind mole fractions
265 from area sources using the bLs model. We measured downwind mole fractions before and after releasing each trace
266 gas, the difference in the mole fractions was then used to determine the source release rate. However, WindTrax cannot
267 be used to carry out backward simulations for point sources (*i.e.* conversion of mole fraction data to fluxes). It can,
268 however, predict downwind mole fraction from estimated release rate using the model running in forward mode.

269 **2.6 Weather data**

270 A three-dimensional (3-D) sonic anemometer (CSAT3, Campbell Scientific, Logan, Utah, US) with data logger
271 (CR5000, Campbell Scientific, Logan, Utah, US) were used to record wind speed and direction along with the
272 turbulence statistics at a frequency of 10 Hz. The fifteen-min interval data were then transformed to friction velocity
273 (u^*), atmospheric stability (L) and surface roughness length (z_0) as half-hour averages, determining the time increments
274 of OP sensor data.

275 **2.7 Data filtering criteria**

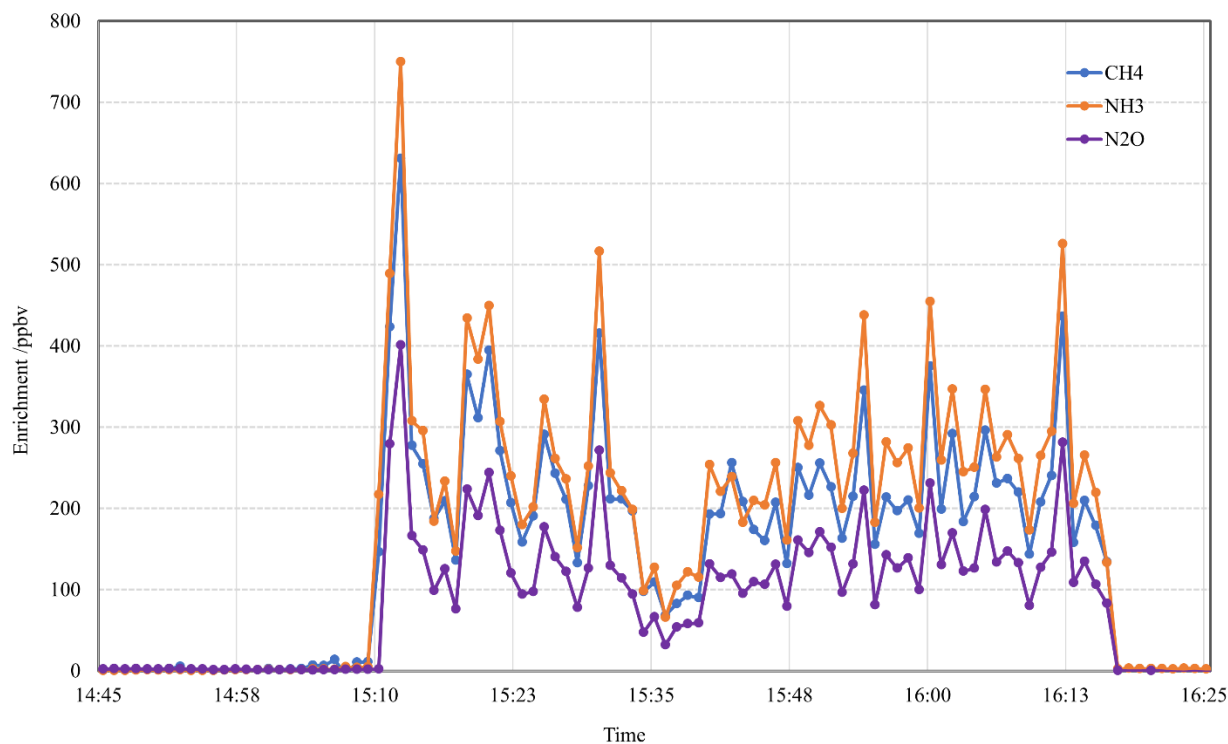
276 Poor measurements of mole fractions were not counted when the spectrum signal intensities were < 0.2 (Spec. max)
277 for OP-FTIR, light level less than 5,000 or greater than 12,000, and $R^2 > 0.90$ for OPL. Following Flesch et al. (2004),
278 we excluded the data that were associated with error-prone WindTrax fluxes (low wind conditions and strong stable
279 or unstable stratification): wind speed $< 2 \text{ m s}^{-1}$, $|L| < 10$, and fraction of “touchdown” < 0.1 .

280 **3 Results and Discussions**

281 **3.1 OP-FTIR measurements**

282 The wind was steady from the NNW ($325\text{-}335^\circ$) at $1.8\text{-}3.5 \text{ m s}^{-1}$ over the measurement period of 14:45-16:30 (local
283 time) on the 27 July 2005 of Kyabram trial (T1). Between 14:45 and 15:10 and after 16:20 background data were
284 collected. Figure 5 shows the OP-FTIR measurements of all three gases during this period, expressed as path-average
285 mole fractions in ppbv after subtracting the background level. We found that the enhanced mole fractions of the source
286 (downwind minus upwind mole fractions) of CH_4 , N_2O , and NH_3 measured by OP-FTIR followed a similar
287 correspondence.

288
289
290



291
 292 **Figure 5: Measured OP-FTIR one-minute average mole fractions of CH₄, N₂O and NH₃ after subtracting the background**
 293 **levels during a point source gas release experiment at Kyabram on 27 July 2005.**
 294

295 We also found that the mean measured OP-FTIR mole fraction of CH₄:N₂O was 1.61 compared to the release rate
 296 ratio of 1.60, and the mean measured mole fraction of NH₃:N₂O was 1.84 (release rate ratio was 1.80). The release
 297 rates with measured regression slopes for all trial release measurements made at both Wollongong and Kyabram are
 298 shown in Table 4. In all but three cases the ratio was within 1–8% of the 1:1 ratio. The OP-FTIR system uses no
 299 calibration gases but system calibration is based on the accuracy of the HITRAN line parameters and the MALT
 300 spectrum model. Typical absolute accuracy is 1–5% depending on species and open path setup, with precision
 301 (reproducibility) normally much better than 1% (Esler et al., 2000). The use of MALT synthetic spectra based on
 302 quantum mechanical parameters has been shown to yield accurate results (within 5% of true amounts) when tested
 303 against calibration gases in a 3.5 L multi-pass gas cell with 24 m optical path length (Smith et al., 2011). In each case
 304 of disagreement, the correlation remains strong, and the systematic differences can reasonably be attributed to either
 305 a leak in the release system or in the case of low NH₃ due to the losses by adsorption at the (wet) ground over the
 306 longer release-measurement distance during the experiment.

307
 308 **Table 4. Comparison of the release rate ratios and OP-FTIR measured enhanced mole fractions for the controlled release**
 309 **gas measurements.**

Location and time of measurement period ^δ	Distance of gas release (m), height of gas release	Compared gases	Ratio of controlled release rates	Ratio of measured enrichments downwind
------------------------------------------------------------	-------------------------------------------------------	-------------------	-----------------------------------------	----------------------------------------------

	(m), measurement path distance (m)		(± 2% measurement error)	(slope of regression ± 95% confidence interval)
Kyabram				
(T1)				
Day 1	10, 0.5, 137	NH ₃ , N ₂ O	1.800 ± 0.036	1.841 ± 0.026
1445–1625 h		CH ₄ , N ₂ O	1.602 ± 0.032	1.609 ± 0.034
Day 2-3	10, 0.5, 137	NH ₃ , N ₂ O	1.000 ± 0.020	1.024 ± 0.010
1730–830 h		CH ₄ , N ₂ O ^{&}	0.890 ± 0.018	0.946 ± 0.038
Day 2	10, 0.5, 137	NH ₃ , N ₂ O	1.000 ± 0.020	1.028 ± 0.019
900–1440 h		CH ₄ , N ₂ O	0.890 ± 0.018	0.873 ± 0.024
Day 2	10, 0.5, 137	NH ₃ , N ₂ O	1.800 ± 0.036	1.990 ± 0.034 [#]
1440–1700 h		CH ₄ , N ₂ O	1.602 ± 0.032	1.668 ± 0.049
(T2)				
Day 1	52, 0.5, 137	NH ₃ , N ₂ O	1.800 ± 0.036	1.783 ± 0.018
1545–1625 h		CH ₄ , N ₂ O	0.890 ± 0.018	0.802 ± 0.025 [#]
Wollongong				
(T3)				
Day 1	44, 1.28, 87.5	NH ₃ , N ₂ O	1.000 ± 0.020	1.009 ± 0.020
2048–0500 h		CH ₄ , N ₂ O	*	*
Day 2	107, 1.28, 150	NH ₃ , N ₂ O	1.000 ± 0.020	0.879 ± 0.019 [#]
2030–0500 h		CH ₄ , N ₂ O	0.890 ± 0.018	0.897 ± 0.032

310 * no data due to CH₄ gas flow problems during this time period.

311 [#] ratio that is not in agreement with the controlled release ratio ($\rho < 0.05$).

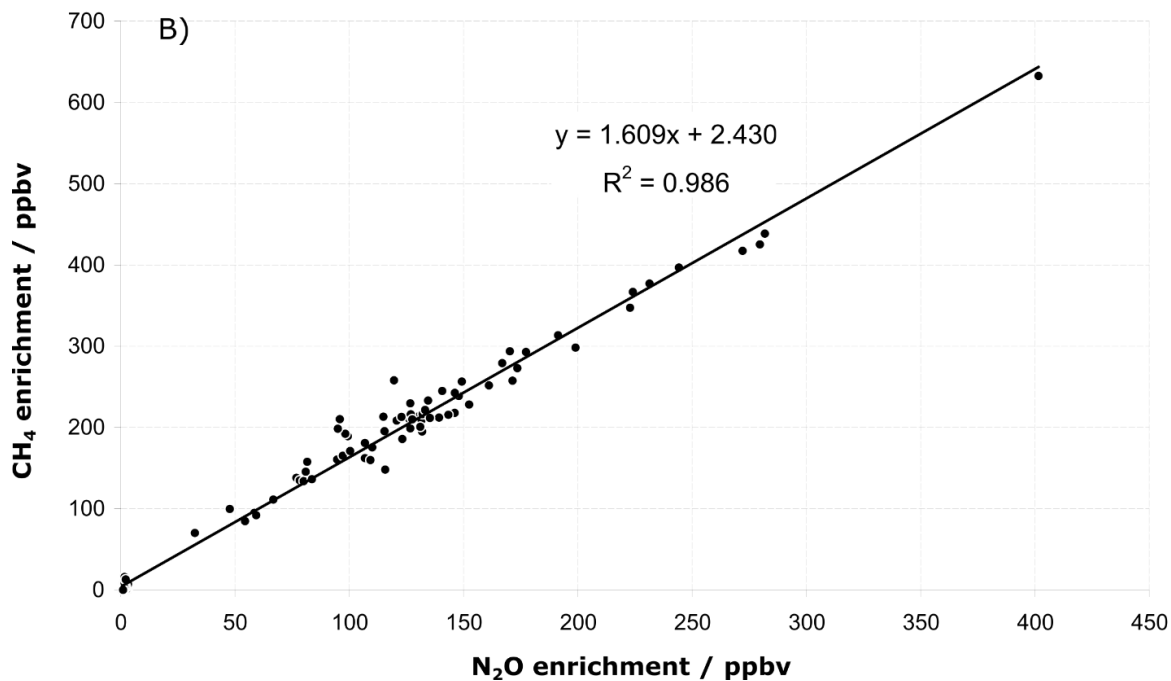
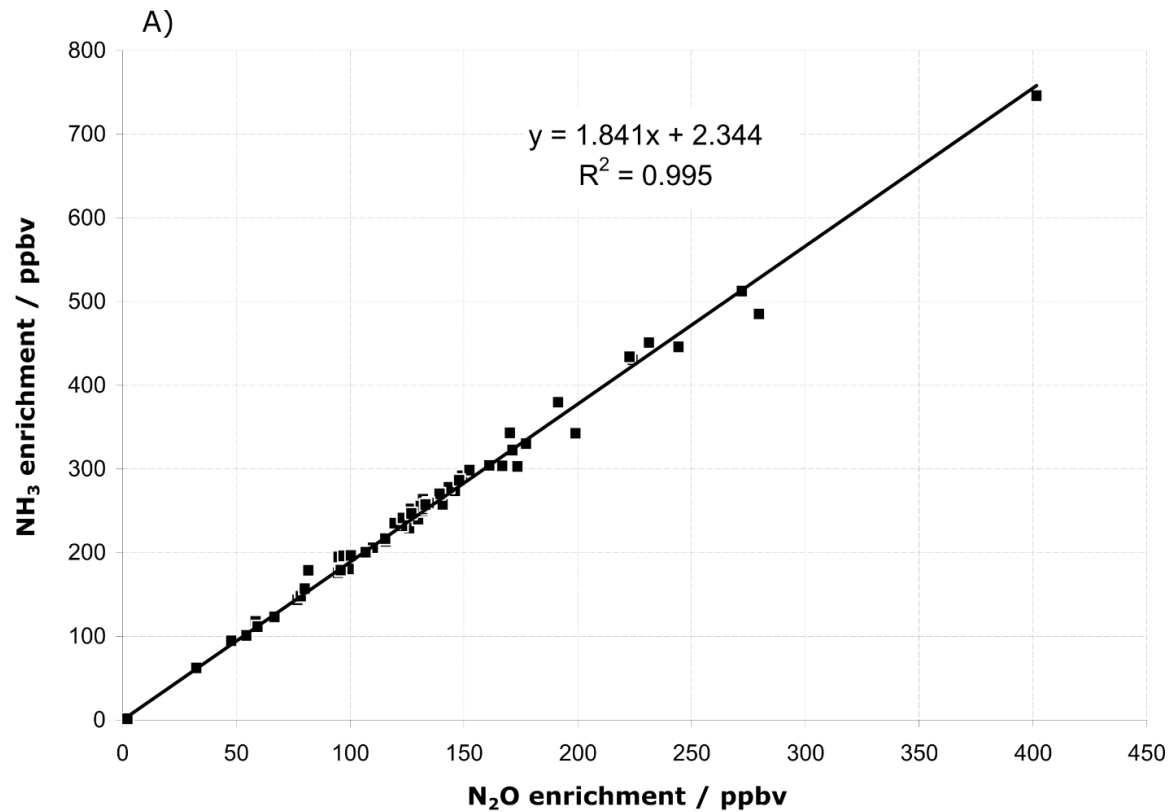
312 ^δ time of measurement period represented local time.

313 [&] the measured mole fraction is from 1730–030 h because of an increased background effect from 030–830 h.

314 3.2 OP-FTIR error assessment

315 From measurements before and after release, the measurement precision and accuracy of the OP-FTIR measurements
316 were assessed (Table 5). Measured background mole fractions of CH₄ and N₂O at Kyabram were similar to the clean
317 air values measured at the Cape Grim Baseline Air Pollution Station in Tasmania. The differences between measured
318 background values at Kyabram and Cape Grim were < 3% and consistent with the known absolute uncertainty in OP-
319 FTIR calibration (1–5%, the accuracy of MALT and HITRAN).

320
321 Regression analyses showed a residual scatter (standard deviation of the residuals) around the regression line of
322 typically 8 ppbv for NH₃:N₂O and 18 ppbv for CH₄:N₂O (Fig. 6). This scatter was significantly larger than the
323 measurement precisions (Table 5) and suggested that the fundamental limit to accuracy and applicability of the OP
324 technique came from variability in the dispersion of the trace gases by atmospheric turbulence – *i.e.*, even when co-
325 released at nominally the same point, statistical fluctuations ensured that gas parcels did not follow exactly the same
326 paths. It thus appeared that measurement precision was not the limiting factor and was sufficient for the purposes of
327 the measurements. Background variations and turbulence statistics were the error-limiting factors in the OP
328 measurements.



329

330 **Figure 6: Regression/correlation analysis of the OP-FTIR measured enrichments shown in Figure 5 between 14:45 and**
 331 **16:25 of NH_3 vs N_2O (A) and CH_4 vs N_2O (B).**

332

333 **Table 5. Measurement precision and comparison with clean air composition for OP-FTIR measurements during the trace**
 334 **gas release trial experimental period at Kyabram. Background mole fractions measured at Cape Grim Baseline Air**
 335 **Pollution Station in Tasmania at the same time are also shown.**

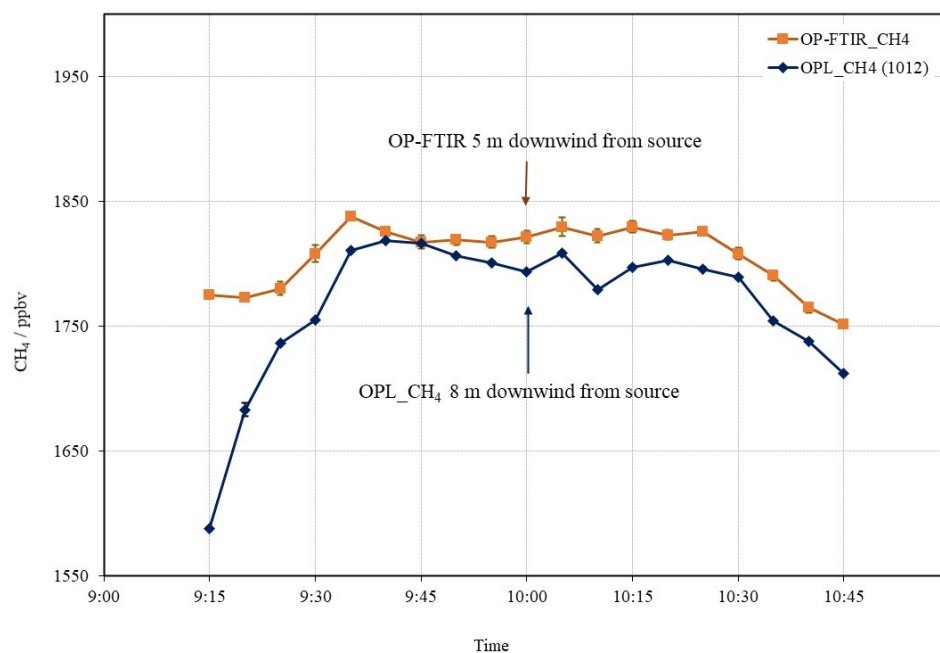
Target gas	Background measured at Cape Grim	Background measured at Kyabram	Precision typical 1σ for repeated measurements
CH ₄ / ppbv	1738	1745	3.8
N ₂ O / ppbv	317.8	310	0.3
NH ₃ / ppbv	0	< 1	0.4

336 Note: 1σ is standard error.

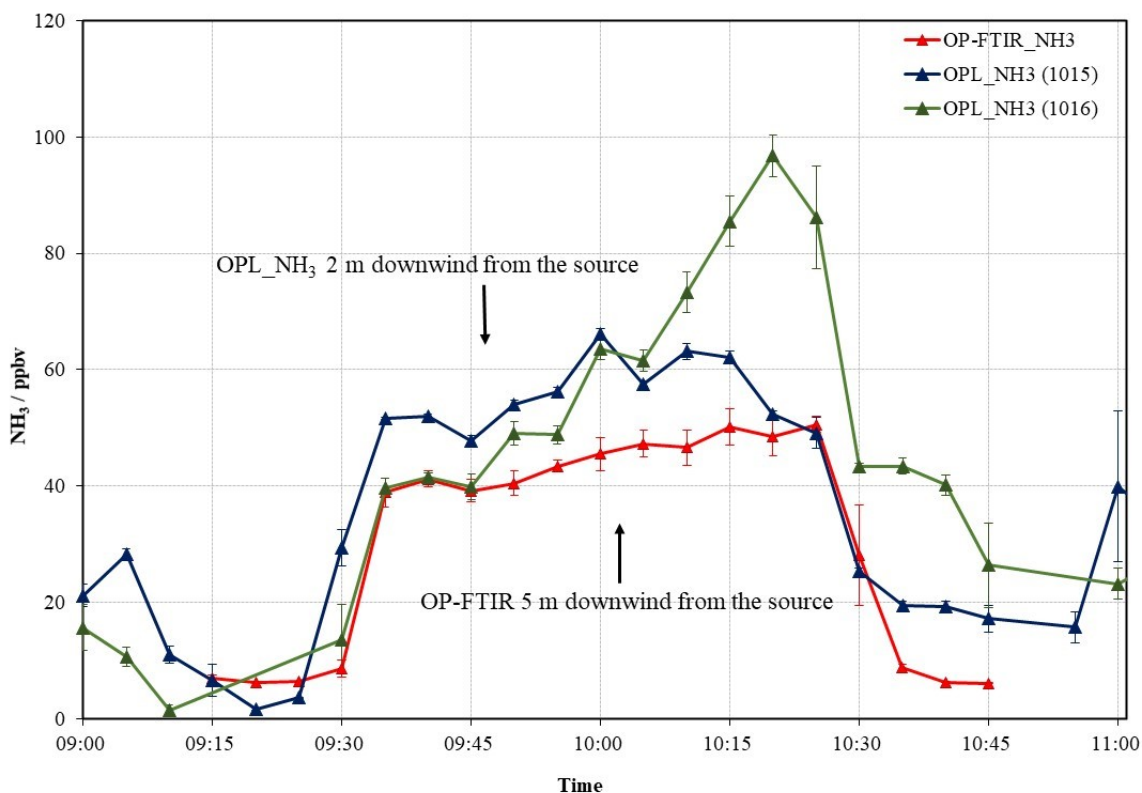
337 3.3 Comparisons of OPL and OP-FTIR measurements

338 The one-minute averages of CH₄ and NH₃ mole fractions measured by OPL (one unit for CH₄, 1012, and two units
339 for NH₃, 1015 and 1016) and the OP-FTIR over the period of controlled gas release at Kyabram (T2) were
340 compared (Fig. 7).

341



342
343
344
345
346
347
348



349
 350 **Figure 7: Five-minute averages of CH₄ (upper) and NH₃ (lower) mole fraction measurements from the OP-FTIR and OPL**
 351 **downwind of a ground-level grid source 40 × 15 m wide (path length = 125 m) at Kyabram on 3 August 2005 (T2). The**
 352 **error bars represent the standard error.**

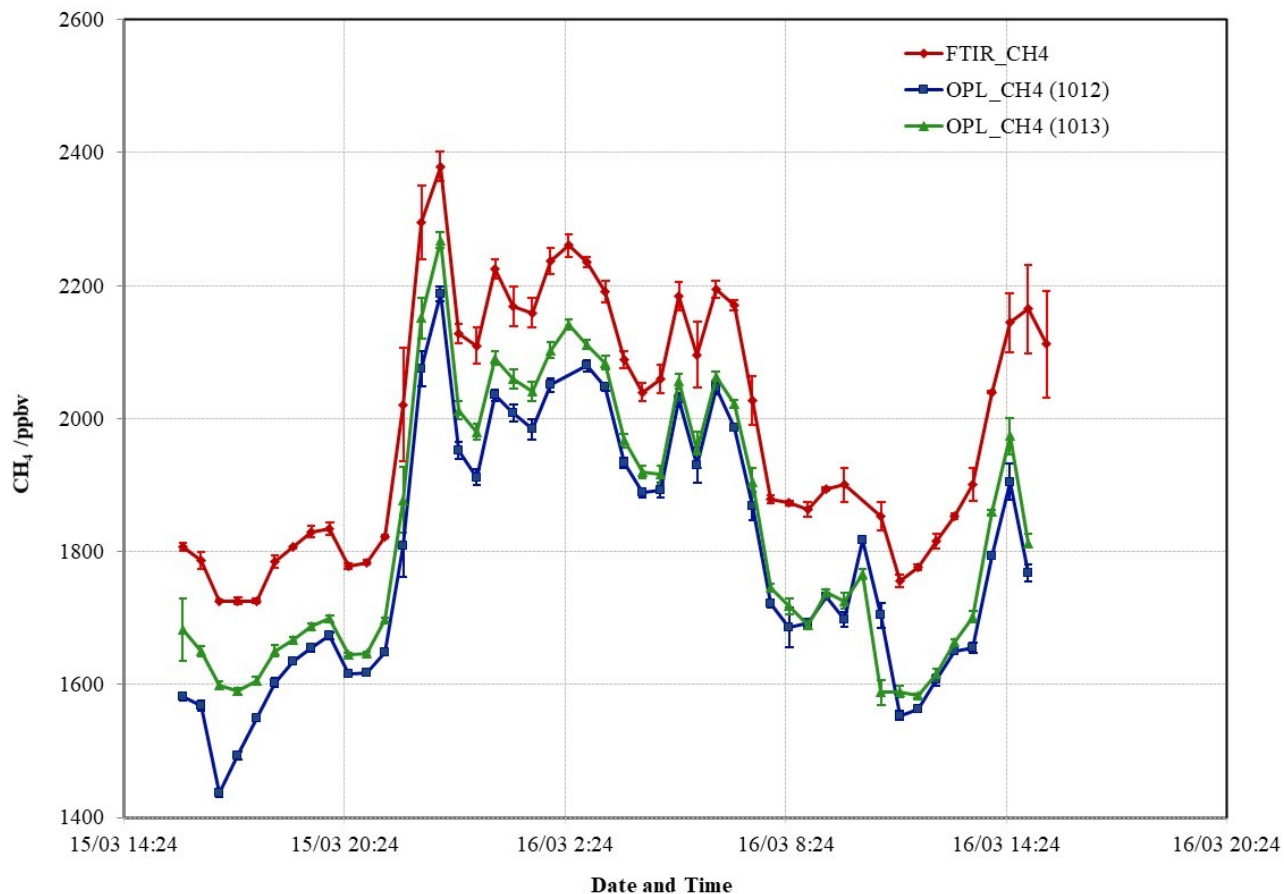
353 In general, the OPL_CH₄ and OPL_NH₃ tracked the OP-FTIR measurements, however, the OPL_NH₃ did not have
 354 a stable baseline (fluctuations of around 15 ppbv) and showed significantly lower signal: noise ratio than that of the
 355 OP-FTIR. Offsets in the measured mole fractions may be due to the relative positions of the emission source and the
 356 instruments.¹

357
 358 A second intercomparison between the CH₄ OPL (1012 and 1013) and OP-FTIR measurements at Wollongong is
 359 shown in Fig. 8. The thirty-minute averaged OPL_CH₄ tracked the OP-FTIR measurements, but recorded lower
 360 values, with background CH₄ lower than the Cape Grim background of 1738 ppbv (Table 5). There were also
 361 discrepancies between the two lasers: 1013 unit was more stable and measured higher values than that of 1012 unit.
 362 Flesch et al. (2004) report a similar problem with the long-term stability of CH₄ lasers and implement a rigorous
 363 calibration strategy, suggesting recalibrating several times over the course of a field campaign. Laubach et al. (2013)
 364 reported the temperature-dependent effect on OPL CH₄ performance. Implementation of a routine calibration protocol

¹ The laser CH₄ mole fractions may be less than those determined by FTIR because the latter's path was only 5 m downwind of the source while the laser path was 8 m downwind. The reverse situation possibly applies to the NH₃ measurements, where the NH₃ laser path was 3 m upwind of that of the FTIR (Fig. 2).

365 would account for these offsets as long as they were consistent. However, fluctuations of around 10 ppbv characterized
366 the limit on the resolution of the instrument.

367

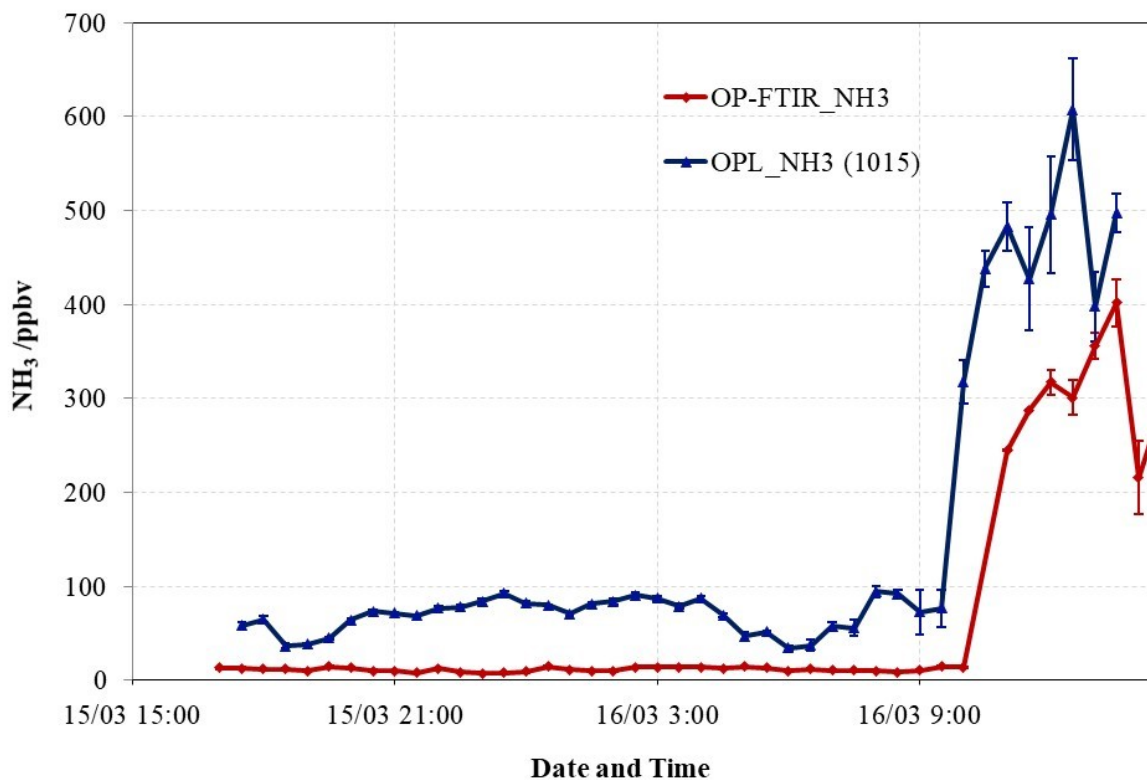


368
369 **Figure 8: Thirty-minute averaged CH₄ mole fraction measured by OP-FTIR and both OPL units (1012 and 1013) positioned**
370 **side-by-side (path length = 148 m) at Wollongong site. Error bars denote the standard error.**

371

372

373



374

375 **Figure 9: Thirty-minute averaged NH₃ mole fraction measured by OP-FTIR and OPL unit (1015) positioned side-by-side**
 376 **(path length = 148 m) at Wollongong site. Error bars denote the standard error of the thirty-minute means.**

377 We also compared thirty-minute averages of NH₃ measurements at Wollongong (Fig. 9) prior to and after the gas
 378 release (NH₃ release rate at 5 L min⁻¹). Prior to the gas release (15 March 2006), the laser mole fractions at background
 379 levels appear elevated while the FTIR showed greater stable baseline, this suggested clearly that the resolution of the
 380 lasers was no better than the 1 ppmv-m specified by the manufacturer. After the NH₃ was released (after 10 am 16
 381 March 2006), the path-averaged mole fraction rose above 0.1 ppmv, but the OPL_NH₃ (1015 unit) measurements were
 382 less erratically at these elevated mole fractions. This indicated the detection limit of the OPL_NH₃ was no better than
 383 the 1 ppm-m specified by the manufacturer. Rigorous calibration should account for between OPL offsets. However,
 384 there remained major discrepancies between measured mole fractions of the OPL_NH₃ and OP-FTIR. Clearly, this
 385 reflected that the OPL_NH₃ are not suited to monitoring background mole fractions of NH₃ (typically < 10 ppbv).
 386 Moreover, they are only likely to be feasible in situations where there are very large enrichments in NH₃ as the
 387 precision is no better than 10 ppbv over 100–200 m paths.

388 3.4 Comparisons of two OP-FTIR spectrometers

389 The ratios of measurement between air samples and FTIR (Bomem and Bruker) are shown in Table 6. We found that
 390 CH₄ results from Bruker FTIR were more reliable in stable conditions than N₂O values, but comparable in Bomem
 391 FTIR results. We also calculated the measurement precisions over a Bruker IRCube which showed higher measurement
 392 precision of CH₄ and N₂O than Bomem MB100, but similarity in NH₃ precision (Table 7).

393
 394 **Table 6. Ratios of mole fractions of CH₄ and N₂O between air samples and OP-FTIR including Bomem MB100 and Bruker**
 395 **IRcube spectrometer[#].**

	CH ₄ _air/ CH ₄ _FTIR	N ₂ O_air/ N ₂ O_FTIR
Bomem MB100	0.99 (0.03)	1.01 (0.03)
Bruker IRcube	1.00 (0.03)	1.04 (0.02)

396 [#]mean (standard deviation). The measurements were conducted at stable background conditions for 6 days at Charlton, Victoria.
 397 The pathlength was 100 m (two-way path), and measurement height was 1.5 m above ground level.
 398

399 **Table 7. The precisions of CH₄, N₂O, and NH₃ for OP-FTIR Bomem MB100 and Bruker IR cube spectrometer.**

	<i>Bomem</i>	<i>Bruker</i>
Precision [#]		
CH ₄	4 ppbv	< 2 ppbv
N ₂ O	0.3 ppbv	< 0.3 ppbv
NH ₃	0.4 ppbv	0.4 ppbv

400 [#] measured over 100 m path length (two-way path).
 401

402 3.5 Trace gas recoveries with Windtrax

403 404 3.5.1 OP-FTIR

405 We ran Windtrax bLs model to calculate trace gas fluxes during a period in the middle of the day on 2 August 2005
 406 with source 3 (25 × 25 m) and path 1 with the mole fraction measured by the OPL (NH₃ only) and OP-FTIR (Fig. 2).
 407 Meteorological conditions varied significantly throughout the period, from unstable ($L \cong -10$ m) at the start to slightly
 408 stable ($L \cong 50$ m) towards the end. Wind speed averaged 2.5 m s⁻¹ and direction was relatively constant at 30°. We
 409 assumed the background mole fraction was constant, 1755, 324, and < 1 ppbv for CH₄, N₂O, and NH₃, respectively
 410 (Table 5). The results of the Windtrax bLs recovery of flux using OP-FTIR mole fractions are illustrated in Appendix
 411 Figure A1 as the ratio of calculated (Q_{bLS}) to known (Q) flux. Recoveries of N₂O flux were generally good, although
 412 low (average recovery is 0.93). This may be due to an issue with the operation of the grid source (such as the
 413 distribution of gas). NH₃ recovery was even lower (mean of 0.71). In this case the adsorption of NH₃ on to the grass
 414 may also contributed to a reduction in measured mole fraction (Tonini 2005). Apart from the first thirty-minute period,
 415 which appeared to have been affected an elevated background mole fraction, CH₄ flux recoveries were much lower
 416 (mean of 0.52) than for the other gases.

417
 418 We also calculated trace gas fluxes with area source 4 (40 × 15 m) and path 2 (Fig. 2). Low release rates were
 419 employed, until the final hour when they were increased by an order of magnitude. Meteorological stability was quite
 420 high at the start of the period ($L \cong 0-10$), gradually becoming less stable during the night and into morning. Wind

421 speed was correspondingly low (1.5 m s^{-1}) at the start and increased to 4 m s^{-1} by the end of the period and wind
422 direction swung from ENE to NNE. The results for N_2O are shown in Appendix Figure A2 and for CH_4 and NH_3 in
423 Appendix Figure A3. The results for the N_2O fluxes were very encouraging. There were some intervals where
424 retrievals were greater than 1 at the start of the period, and 2 towards the end. The latter occurred at a time when wind
425 speed increased, and conditions swung from neutral to unstable. Excluding these intervals provided an average ratio
426 of 1.04, with a standard deviation of 0.15. Few points were available for NH_3 as it was not released during the night.
427 The average for the last two data points was 0.96. Once again, CH_4 retrievals were problematic due to variations in
428 the background mole fraction. With this source geometry and wind field a change in flux of 1 mmole s^{-1} result in a
429 path averaged change in mole fraction of 50 ppbv. Small variations in the background thus translated to large mass
430 flux changes (e.g. 1 ppb corresponds to $1/50 \text{ mmole s}^{-1} = 0.32 \text{ mg s}^{-1}$, or 5.8 % of the released flux of 5.5 mg s^{-1}).
431 Under these conditions accurate flux calculation requires a well-defined background mole fraction measurement.

432 3.5.2 Lasers (NH_3)

433 Figure A4 showed the results of the same controlled release experiment described in the OP-FTIR section above.
434 Again, the bLs model was used to predict the NH_3 emission source strength based on OPL NH_3 line-averaged mole
435 fraction measurements.

436

437 Although the correlation was reasonable, unlike the recoveries calculated from the OP-FTIR data, the ratio of predicted
438 to known source strength was greater than 1 for these data. This was not altogether surprising given the consistently
439 inflated NH_3 mole fractions measured by the OPL sensors.

440 3.6 Herd emissions using OP-FTIR, OPL and WindTrax

441 The study was conducted at Kyabram DPI on March 21, 2006 (Appendix Figure 5A). Appendix Figures A6 and A7
442 showed the fluxes of CH_4 and NH_3 due to a herd of 353 dairy cows grazing at Kyabram DPI on March 21, 2006,
443 calculated using bLs model in WindTrax and OP-FTIR and OPL (for CH_4) measured mole fractions. The calculated
444 CH_4 source was variable because the cows were wandering around the paddock (Fig. A6). Clearly marked at the time
445 when the cows departed the bay (Bay 8) for milking. The CH_4 source strength disappeared after this time, as it should.
446 Missing data points corresponded to periods of time when the average wind speed was less than 2 m s^{-1} , when the bLs
447 model was likely unreliable. The average calculated source strength, based on the OP-FTIR data, was $57.5 \mu\text{g m}^{-2} \text{ s}^{-1}$,
448 equivalent to $292 \text{ g cow}^{-1} \text{ day}^{-1}$. This calculation assumed a uniform background mole fraction of CH_4 of 1610 ppbv.
449 Fluxes based on the upwind and downwind OPL data were strongly correlated with the OP-FTIR results and predicted
450 an average flux of $48.5 \mu\text{g m}^{-2} \text{ s}^{-1}$. The lower value probably reflected the offsets between the instruments. Atmospheric
451 conditions of the following day were too still to reliably use the data acquired on the second day of grazing. Figure
452 A7 showed that the OP-FTIR NH_3 fluxes ranged from $0.3\text{-}0.8 \mu\text{g m}^{-2} \text{ s}^{-1}$, with average flux around $0.5 \mu\text{g m}^{-2} \text{ s}^{-1}$,
453 equivalent to $0.7 \text{ gN cow}^{-1} \text{ day}^{-1}$ assuming NH_3 volatilisations only occurred during the daytime (8 hours). This was
454 similar to the NH_3 emission fluxes of 0.25 to $2.5 \text{ g cow}^{-1} \text{ day}^{-1}$, measured at the same site and same season (early
455 April) in 2004 using the combination of passive NH_3 sampler and WindTrax (Denmead et al., 2020).

456 3.7 WindTrax sensitivity

457 A model sensitivity study was undertaken in order to understand how the source strength predicted by WindTrax alters
 458 with variations in a range of input parameters. No sonic anemometer data was used – instead we used simple wind
 459 speed and direction and constructed a surface layer model from local weather conditions and estimates of surface
 460 roughness. Example data from FTIR measurements in Kyabram on 21 March 2006 was used and five input parameters
 461 were varied around the standard conditions. Table 8 below showed how the calculated source strength of CH₄ from
 462 the paddock of cows varied with changes in the wind speed, stability, surface roughness, height of sensor and
 463 temperature assumed by the WindTrax model.

464 **Table 8. Variations in input parameters to WindTrax.**

Wind Speed	1.00 m s ⁻¹	2.00 m s ⁻¹	2.67 m s⁻¹	3.00 m s ⁻¹	4.00 m s ⁻¹	
Source strength (µg m ⁻² s ⁻¹)	32 ± 4	64 ± 9	85 ± 11	96 ± 13	128 ± 17	
Stability	Bright sunshine	Moderate sunshine	Slight sunshine	Overcast	night < 3/8 cloud	night > 4/8 cloud
Source strength (µg m ⁻² s ⁻¹)	85 ± 11	74 ± 10	74 ± 10	74 ± 10	74 ± 10	74 ± 10
Surface Roughness	2.3 cm	5 cm	10 cm	12 cm	15 cm	
Source strength (µg m ⁻² s ⁻¹)	64 ± 9	64 ± 8	85 ± 11	85 ± 11	85 ± 11	
Height of Sensor	1.4 m	1.5 m	1.6 m	1.8 cm		
Source strength (µg m ⁻² s ⁻¹)	88 ± 8	85 ± 11	81 ± 12	78 ± 7		
Temperature	15°C	20°C	22°C	24°C	30°C	
Source strength (µg m ⁻² s ⁻¹)	87 ± 12	86 ± 11	85 ± 11	85 ± 11	83 ± 11	

468
 469
 470 The model appeared to be quite robust with respect to height of the sensor, temperature and stability conditions while
 471 changing the assumed surface roughness from 5 to 10 cm altered the predicted fluxes quite markedly. The modelled
 472 source strength scaled with wind speed so accurate meteorological data was a requirement of this technique. It should
 473 also be noted that the Windtrax model was not expected to work well when wind speed was below 2 m s⁻¹.

474 3.8 The total uncertainty budget

475 We want to compute the total uncertainty associated with the difference in mole fraction between upwind and
 476 downwind. There are three uncertainty sources: instrument precision uncertainty, fitting uncertainty, and absorption
 477 cross-section (HITRAN) uncertainty (the latter two are fractional uncertainties and were taken from Paton-Walsh et
 478 al.(2014)) (Table 9). The measurement precision is in units of ppbv and so the fractional uncertainty that this represents
 479 will change with the trace gas mole fraction. The instrument precision uncertainty (δ) associated with upwind
 480 measurement is $1-\sigma$, and the uncertainty associated with downwind is also $1-\sigma$. We assume these errors to be
 481 independent. The instrument precision uncertainty in the difference in mole fraction between upwind and downwind
 482 is thus $\sqrt{((1-\sigma)^2 + (1-\sigma)^2)}$. We then divide this value by the difference in mole fraction to recover the relative
 483 uncertainty due to instrument precision: $\sqrt{((1-\sigma)^2 + (1-\sigma)^2)} / (\text{CH}_4_{\text{downwind}} - \text{CH}_4_{\text{upwind}})$. $\Delta\text{CH}_4 = \text{CH}_4_{\text{downwind}} -$
 484 $\text{CH}_4_{\text{upwind}}$. We then add in quadrature the relative measurement uncertainty due to instrument precision with the fitting

485 and absorption cross-section uncertainties (also expressed in terms of relative uncertainty). For example, for CH₄,
 486 when ΔCH₄ was as low as 20 ppbv, we have a relative uncertainty of 0.28 for the instrument precision, 0.02 for fitting
 487 uncertainty, and 0.05 for absorption cross-section uncertainty. The relative uncertainty propagated across these three
 488 components is: $\sqrt{0.283^2 + 0.02^2 + 0.05^2} = 0.288$ or 28.8%. When the ΔCH₄ was increased to 50 ppbv or 100
 489 ppbv, the uncertainty declined dramatically to 12.5 and 7.8%, respectively. However, for N₂O and NH₃ the uncertainty
 490 was not limited by the mole fraction enhancement but likely attributed to absorption cross-section uncertainty.

491 **Table 9. Total uncertainty budget.**

	CH ₄	N ₂ O	NH ₃
Measurement precision (ppbv)	4	0.3	0.4
Spectral fitting uncertainty (%)	2%	4%	2%
Absorption cross-section uncertainty (%)	5%	5%	5%
$\delta(\Delta \text{ trace gas mole fraction}^\ddagger)/\Delta \text{ trace mole fraction (\%)}$			
$\Delta \text{ trace gas mole fraction (ppbv)}$			
20	28.3%	2.1%	2.8%
50	11.3%	0.8%	1.1%
100	5.7%	0.4%	0.6%
Total uncertainty (%)			
$\Delta \text{ trace gas mole fraction (ppbv)}$			
20	28.8%	6.8%	6.1%
50	12.5%	6.5%	5.5%
100	7.8%	6.4%	5.4%

492 $^\ddagger \Delta \text{ trace gas mole fraction} = (\text{trace gas mole fraction})_{\text{downwind}} - (\text{trace gas mole fraction})_{\text{upwind}}$

493 **4 Conclusions**

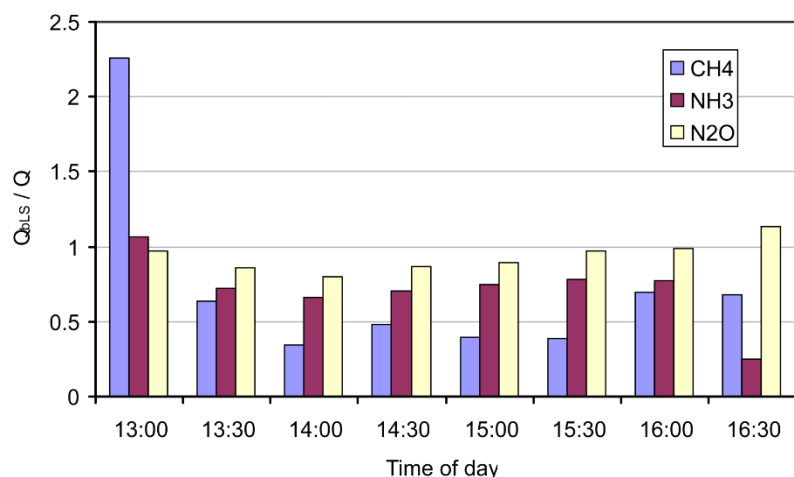
494 We have used OP systems for measuring mole fractions of CH₄, N₂O and NH₃, and evaluated their performance and
 495 precision. Two OP systems for measuring line-averaged gas mole fractions have been evaluated over path lengths up
 496 to about 200 m.

497
 498 The OP-FTIR system can measure multiple gases simultaneously with excellent precision, e.g., CH₄, 2-4 ppbv, N₂O,
 499 0.3 ppbv, and NH₃, 0.4 ppbv. As the baseline appears to be very stable, we believe OP-FTIR technique has accuracy
 500 for even small enrichments in GHGs. However, the apparatus remains bulky to set up in a field environment, where
 501 access to main power is often difficult. In contrast, the commercial OPL have the advantage of being readily portable
 502 and battery powered. This study has evaluated OPL for CH₄ and NH₃. These instruments have somewhat poorer
 503 precision than the OP-FTIR, of around 10 ppbv for CH₄ and 15 ppbv for NH₃. While the OPL should be capable of
 504 following ambient fluctuations in CH₄ gas mole fractions, the resolution of the NH₃ OPL was greater than the
 505 background mole fractions of NH₃, resulting in large errors when calculating fluxes. WindTrax provided accurate
 506 recoveries of known test gas releases from source area and appears to be well suited to analysis of open path
 507 measurements, under suitable meteorological conditions. These experiments highlighted the importance of having a
 508 robust background mole fraction measurement.

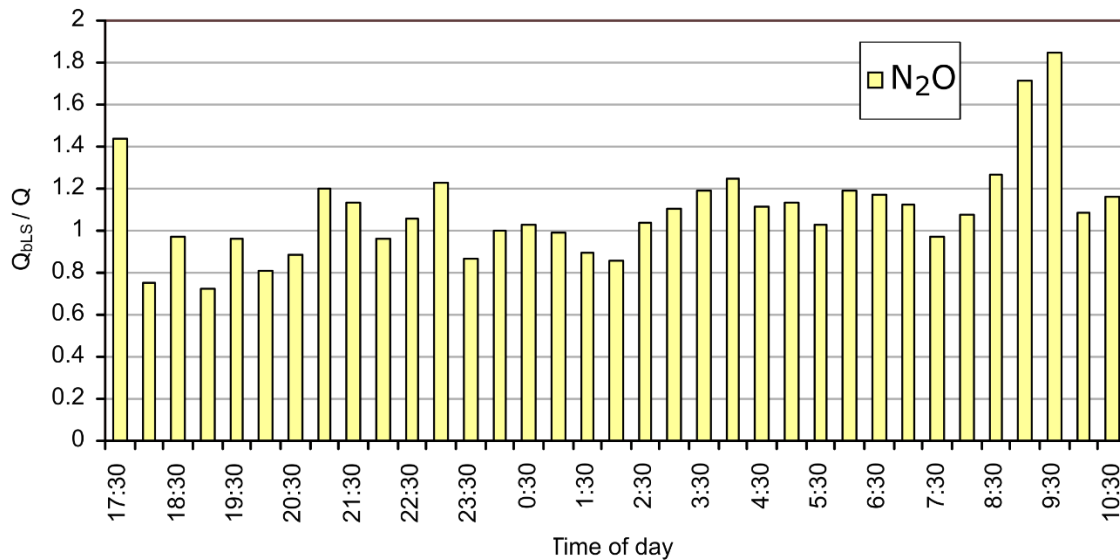
509
 510 Our studies also suggest that the OP-FTIR and OPL are suitable to measure typical enrichments in CH₄ and NH₃ from
 511 agriculture and useful in calculating fluxes from a variety of agricultural activities, such as free-ranging cattle and
 512 sheep. We recommend that they are also well-suited to concentrated sources such as feedlots, animal sheds and small
 513 enclosures. The OP-FTIR system should also be suited to emissions of CH₄ from rice-growing sources and wastewater
 514 lagoons. The OP-FTIR system provides excellent NH₃ precision suitable for measuring paddock-scale emissions from
 515 fertiliser (urea, effluent) applications and dung and urine patches. High detection limit and long-term stability of OP-
 516 FTIR enables to measure small changes in N₂O emissions at large-scale from fertilizer treatment, or dairy pastures.
 517 The OPL NH₃ has low resolution of free-air mole fraction, in particular weak sources, where the enhanced values are
 518 low and the error in background is minimized.

519 **5 Appendices**

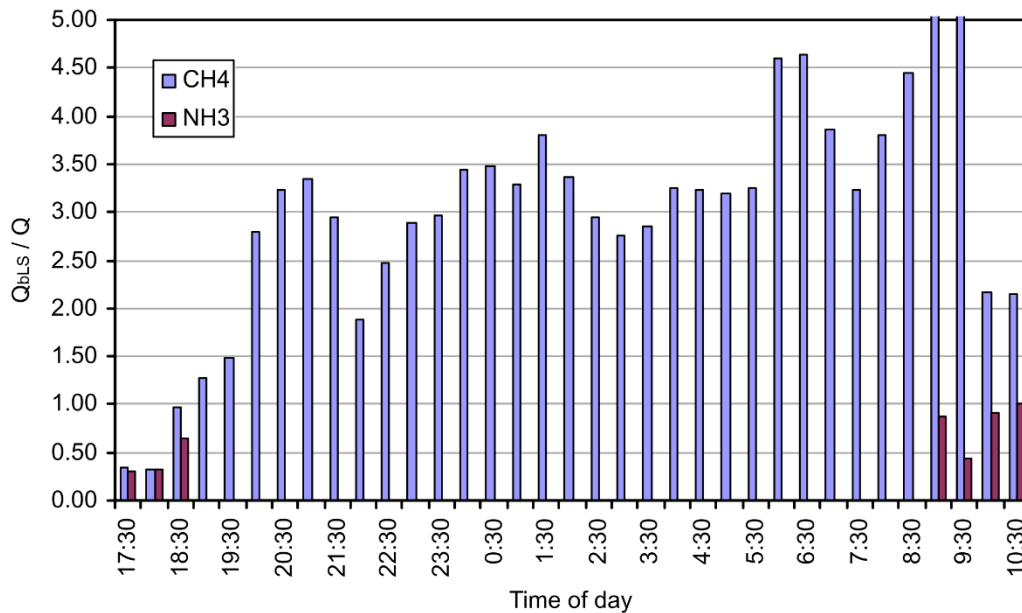
520 Appendix A



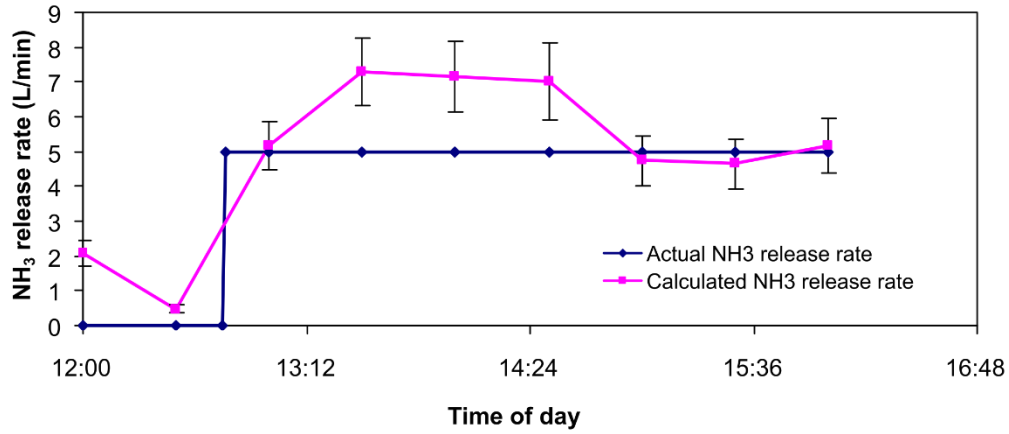
521
 522
 523 **Figure A1: Ratio of predicted to known flux for ground-level 25 × 25 m area source (Source 3), using OP-FTIR mole**
 524 **fractions and measurement path 2 on 2 August 2005.**
 525
 526



527
 528 **Figure A2: Ratio of calculated (Q_{bLS}) to known N_2O (Q) fluxes for the ground-level 40×25 m grid source (Source 4),**
 529 **using OP-FTIR mole fractions and measurement path 2.**
 530

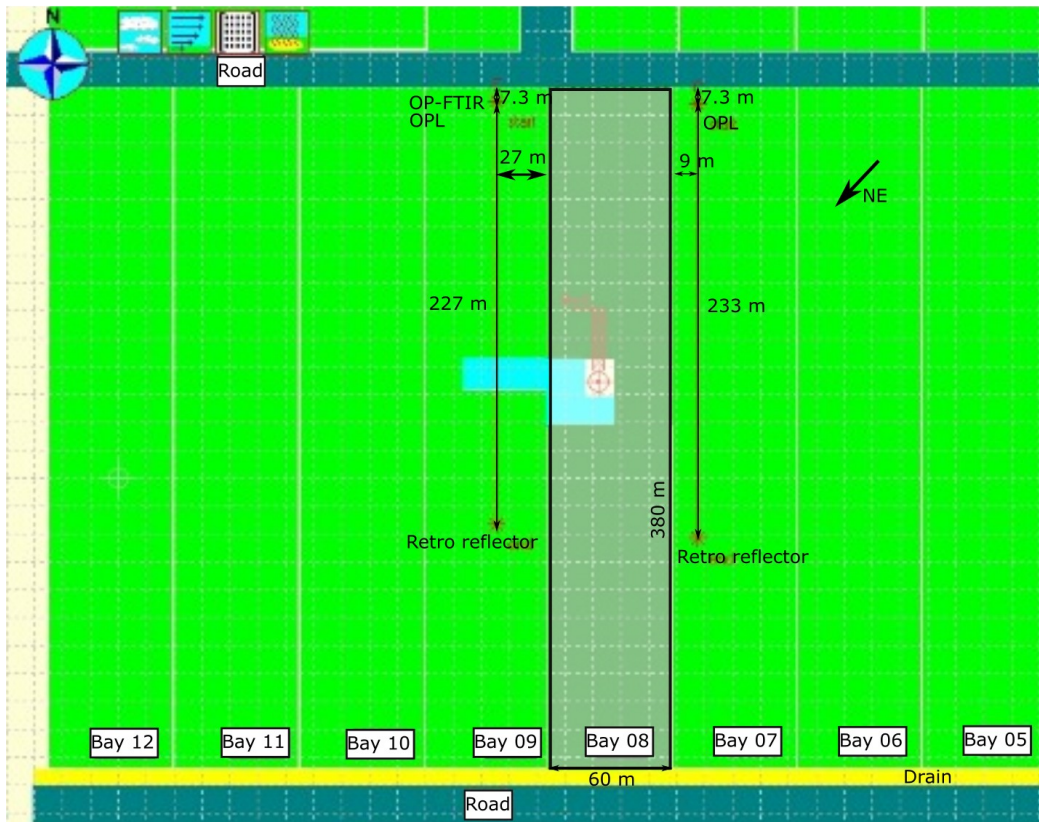


531
 532 **Figure A3: Ratio of calculated (Q_{bLS}) to known CH_4 and NH_3 (Q) fluxes for the ground-level 40×25 m grid source (Source**
 533 **4), using OP-FTIR mole fractions and measurement path 2.**
 534



535
536
537
538

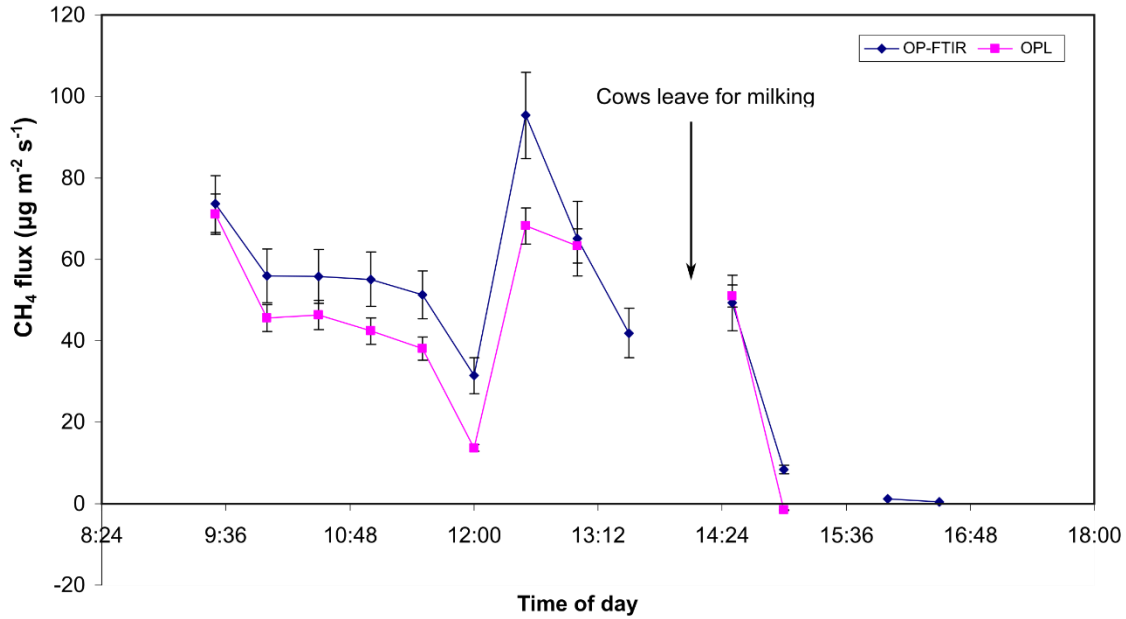
Figure A4: Controlled release from 25 x 25 m grid (Source 3). Calculated release was average of bLs WindTrax calculations using line-averaged mole fraction measurements from two NH₃ lasers.



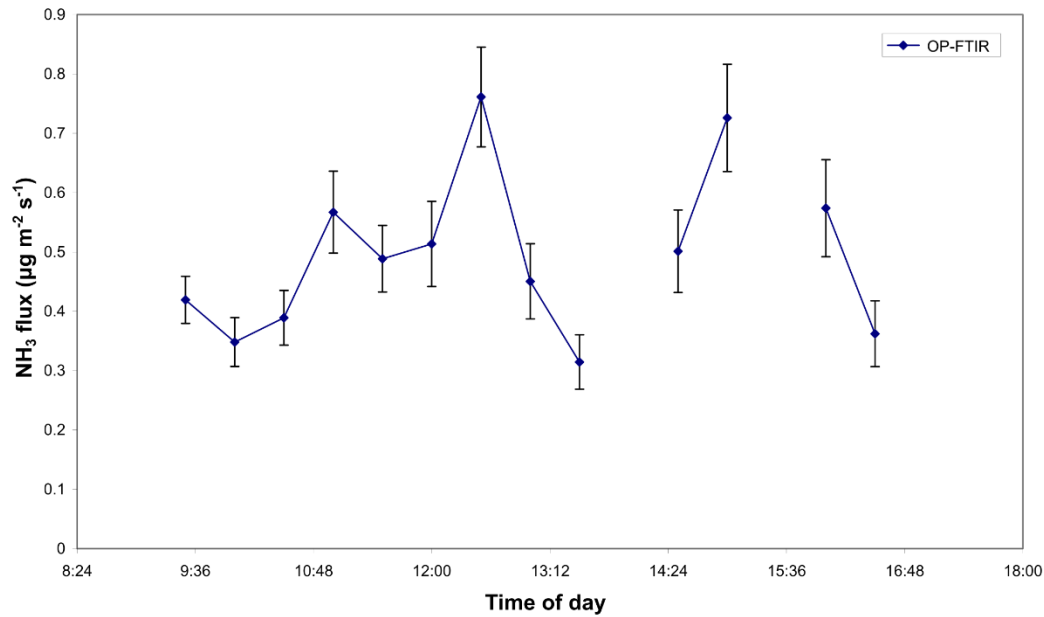
539
540

Figure A5: A WindTrax map showing the layout of herd emissions study at Kyabram on 21 March 2006.

541



542
543 **Figure A6: CH₄ fluxes determined from OP-FTIR and OPL (1012) data and the bLs model at Kyabram 21 March 2006.**



544
545 **Figure A7: NH₃ fluxes determined from OP-FTIR data and the bLs model in WindTrax at Kyabram 21 March 2006.**
546

547 **6 Data availability**

548 The raw data are not available to the public. For any inquiry about the data, please contact the corresponding author
549 (mei.bai@unimelb.edu.au).

550 **7 Author contributions**

551 All authors contributed to the conceptualization, methodology, field measurement, data analysis, and draft preparation.

552 **8 Acknowledgements**

553 We wish to acknowledge the assistance of many: Ron Teo from the University of Melbourne, the Victorian Kyabram
554 research station for access to their laboratory and experimental facilities, for provision of micrometeorological data at
555 Kyabram, and the assistance of their staff, particularly Kevin Kelly, Rob Baigent. We wish to thank also the Australian
556 Greenhouse Office for their encouragement. Authors would like to thank Travis Naylor, Graham Kettlewell from
557 University of Wollongong for their assistance during this study.

558 **9 Declaration of interests**

559 The authors declare that they have no known competing financial interests or personal relationships that could have
560 appeared to influence the work reported in this paper.

561 **10 References**

- 562 Bai, M.: Methane emissions from livestock measured by novel spectroscopic techniques, Doctor of Philosophy PhD
563 Thesis, School of Chemistry, University of Wollongong, University of Wollongong, NSW, Australia, 303 pp., 2010.
- 564 Bai, M., Flesch, K. T., Trouvé, R., Coates, T. W., Butterly, C., Bhatta, B., Hill, J., and Chen, D.: Gas Emissions
565 during Cattle Manure Composting and Stockpiling, *J. Environ. Qual.*, 49, 228-235,
566 <https://doi.org/10.1002/jeq2.20029>, 2020.
- 567 Bai, M., Flesch, T., McGinn, S., and Chen, D.: A snapshot of greenhouse gas emissions from a cattle feedlot, *J.*
568 *Environ. Qual.*, 44, 1974-1978, <https://doi.org/10.2134/jeq2015.06.0278>, 2015.
- 569 Bai, M., Sun, J., Dassanayake, K. B., Benvenuti, M. A., Hill, J., Denmead, O. T., Flesch, K. T., and Chen, D.: Non-
570 interference measurement of CH₄, N₂O and NH₃ emissions from cattle, *Anim. Prod. Sci.*, 56, 1496-1503,
571 <https://doi.org/10.1071/AN14992>, 2016.
- 572 Bjorneberg, L. D., Leytem, B. A., Westermann, T. D., Griffiths, R. P., Shao, L., and Pollard, J. M.: Measurement of
573 atmospheric ammonia, methane, and nitrous oxide at a concentrated dairy production facility in Southern Idaho
574 using open-path FTIR Spectrometry, *Trans. of the ASABE*, 52, 1749-1756, <https://doi.org/10.13031/2013.29137>,
575 2009.
- 576 Bühler, M., Häni, C., Kupper, T., Ammann, C., and Brönnimann, S.: Quantification of methane emissions from
577 waste water treatment plants, 13389, 2020.
- 578 Crenna, B., Thomas, K. F., and Wilson, J. D.: WindTrax 2.0.6.8 (06 12 04). Alberta Canada, 2006.
- 579 de Klein, C., Novoa, R. S. A., Ogle, S., Smith, K. A., Rochette, P., Wirth, T. C., McConkey, B. G., Mosier, A., and
580 Rypdal, K.: N₂O emissions from managed soils, and CO₂ emissions from lime and urea application. In: 2006 IPCC
581 Guidelines for National Greenhouse Gas Inventories Volume 4 Agriculture, Forestry and Other Land Use,
582 Eggleston, S., Buendia, L., Miwa, K., Ngara, T., and Tanabe, K. (Eds.), Cambridge University Press, Cambridge,
583 United Kingdom and New York, NY, USA., 2006.
- 584 Denmead, O. T.: Novel meteorological methods for measuring trace gas fluxes, *Philos. T. R. Soc. A.*, 351, 383-396,
585 1995.
- 586 Denmead, O. T., Bai, M., Turner, D., Li, Y., Edis, R., and Chen, D.: Ammonia emissions from irrigated pastures on
587 Solonetz in Victoria, Australia, *Geoderma Regional*, 20, e00254, <https://doi.org/10.1016/j.geodrs.2020.e00254>,
588 2020.
- 589 Denmead, O. T., Harper, L. A., Freney, J. R., Griffith, D. W. T., Leuning, R., and Sharpe, R. R.: A mass balance
590 method for non-intrusive measurements of surface-air trace gas exchange, *Atmos. Environ.*, 32, 3679-3688, 1998.
- 591 Esler, M. B., Griffith, D. W. T., Wilson, S. R., and Steele, L. P.: Precision trace gas analysis by FT-IR Spectroscopy.
592 I. Simultaneous analysis of CO₂, CH₄, N₂O, and CO in Air, *Anal. Chem.*, 72, 206-215,
593 <https://doi.org/10.1021/ac9905625>, 2000.
- 594 Feitz, A., Schroder, I., Phillips, F., Coates, T., Negandhi, K., Day, S., Luhar, A., Bhatia, S., Edwards, G., Hrabar, S.,
595 Hernandez, E., Wood, B., Naylor, T., Kennedy, M., Hamilton, M., Hatch, M., Malos, J., Kochanek, M., Reid, P.,
596 Wilson, J., Deutscher, N., Zegelin, S., Vincent, R., White, S., Ong, C., George, S., Maas, P., Towner, S., Wokker,
597 N., and Griffith, D.: The Ginninderra CH₄ and CO₂ release experiment: An evaluation of gas detection and

598 quantification techniques, *Int. J. Greenh. Gas Control*, 70, 202-224, <https://doi.org/10.1016/j.ijggc.2017.11.018>,
599 2018.

600 Flesch, K. T., Baron, V., Wilson, J., Griffith, D. W. T., Basarab, J., and Carlson, P.: Agricultural gas emissions
601 during the spring thaw: Applying a new measurement technique, *Agric. Forest Meteorol.*, 221, 111-121,
602 <https://doi.org/10.1016/j.agrformet.2016.02.010>, 2016.

603 Flesch, T. K., Desjardins, R. L., and Worth, D.: Fugitive methane emissions from an agricultural biogas digester,
604 *Biomass and Bioenergy*, 35, 3927-3935, <http://dx.doi.org/10.1016/j.biombioe.2011.06.009>, 2011.

605 Flesch, T. K., Vergé, X. P. C., Desjardins, R. L., and Worth, D.: Methane emissions from a swine manure tank in
606 western Canada, *Can. J. Anim. Sci.*, 93, 159-169, <https://doi.org/10.4141/cjas2012-072>, 2012.

607 Flesch, T. K., Wilson, J. D., Harper, L. A., Crenna, B. P., and Sharpe, R. R.: Deducing ground-to-air emissions from
608 observed trace gas mole fractions: A field trial, *J. Appl. Meteorol.*, 43, 487-502, [https://doi.org/10.1175/1520-0450\(2004\)043<0487:DGEFOT>2.0.CO;2](https://doi.org/10.1175/1520-0450(2004)043<0487:DGEFOT>2.0.CO;2), 2004.

609 Flesch, T. K., Wilson, J. D., and Yee, E.: Backward-time Lagrangian stochastic dispersion models and their
610 application to estimate gaseous emissions, *J. Appl. Meteorol.*, 34, 1320-1332, 10.1175/1520-
611 0450(1995)034<1320:BTLSDM>2.0.CO;2, 1995.

612 Griffith, D. W. T.: Synthetic calibration and quantitative analysis of gas-phase FT-IR spectra, *Appl. Spectrosc.*, 50,
613 59-70, 1996.

614 Griffith, D. W. T., Deutscher, N. M., Caldow, C., Kettlewell, G., Riggenbach, M., and Hammer, S.: A Fourier
615 transform infrared trace gas and isotope analyser for atmospheric applications, *Atmos. Meas. Tech.*, 5, 2481-2498,
616 <https://doi.org/10.5194/amt-5-2481-2012>, 2012.

617 Harper, L. A., Flesch, T. K., Powell, J. M., Coblenz, W. K., Jokela, W. E., and Martin, N. P.: Ammonia emissions
618 from dairy production in Wisconsin, *J. Dairy Sci.*, 92, 2326-2337, <https://doi.org/10.3168/jds.2008-1753>, 2009.

619 Harper, L. A., Flesch, T. K., and Wilson, J. D.: Ammonia emissions from broiler production in the San Joaquin
620 Valley, *Poult. Science*, 89, 1802-1814, <https://doi.org/10.3382/ps.2010-00718>, 2010.

621 IPCC: Emissions from managed soils, and CO₂ emissions from lime and urea application. In '2006 IPCC Guidelines
622 for National Greenhouse Gas Inventories. Vol. 4. Agriculture forestry and other land use'. Ch. 11. Prepared by the
623 National Greenhouse Gas Inventories Programme, International Panel on Climate Change, Hayama, Japan, 54 pp.,
624 2006.

625 Laubach, J., Barthel, M., Fraser, A., Hunt, J. E., and Griffith, D. W. T.: Combining two complementary
626 micrometeorological methods to measure CH₄ and N₂O fluxes over pasture, *Biogeosciences*, 13, 1309-1327,
627 <https://doi.org/10.5194/bg-13-1309-2016>, 2016.

628 Loh, Z., Chen, D., Bai, M., Naylor, T., Griffith, D., Hill, J., Denmead, T., McGinn, S., and Edis, R.: Measurement of
629 greenhouse gas emissions from Australian feedlot beef production using open-path spectroscopy and atmospheric
630 dispersion modelling, *Aust. J. Exp. Agr.*, 48, 244-247, 2008.

631 Loh, Z., Leuning, R., Zegelin, S., Etheridge, D., Bai, M., Naylor, T., and Griffith, D.: Testing Lagrangian
632 atmospheric dispersion modelling to monitor CO₂ and CH₄ leakage from geosequestration, *Atmos. Environ.*, 43,
633 2602-2611, 2009.

634 McGinn, S. M.: Measuring greenhouse gas emissions from point sources, *Can. J. Soil Sci.*, 86, 355-371, 2006.

635 McGinn, S. M., Coates, T., Flesch, T. K., and Crenna, B.: Ammonia emission from dairy cow manure stored in a
636 lagoon over summer, *Can. J. Soil Sci.*, 88, 611-615, <https://doi.org/10.4141/CJSS08002>, 2008.

637 McGinn, S. M. and Flesch, T. K.: Ammonia and greenhouse gas emissions at beef cattle feedlots in Alberta Canada,
638 *Agri. Forest Meteorol.*, 258, 43-49, <https://doi.org/10.1016/j.agrformet.2018.01.024>, 2018.

639 McGinn, S. M., Flesch, T. K., Harper, L. A., and Beauchemin, K. A.: An Approach for Measuring Methane
640 Emissions from Whole Farms, *J Environ. Qual.*, 35, 14-20, 10.2134/jeq2005.0250, 2006.

641 NIR: National Inventory Report 2015 Volume I, Commonwealth of Australia 2017. www.environment.gov.au.
642 (updated June 2017). 2015.

643 Paton-Walsh, C., Smith, T. E. L., Young, E. L., Griffith, D. W. T., and Guérette, É. A.: New emission factors for
644 Australian vegetation fires measured using open-path Fourier transform infrared spectroscopy-Part 1: Methods and
645 Australian temperate forest fires., *Atmos. Chem. Phys.*, 14, 11313-11333, <https://doi.org/10.5194/acp-14-11313-2014>, 2014.

646 Phillips, F. A., Naylor, T., Forehead, H., Griffith, D. W. T., Kirkwood, J., and Paton-Walsh, C.: Vehicle Ammonia
647 Emissions Measured in An Urban Environment in Sydney, Australia, Using Open Path Fourier Transform Infra-Red
648 Spectroscopy, *Atmosphere*, 10, 208, 2019.

649 Rothman, L. S., Gordon, I. E., Barbe, A., Benner, D. C., Bernath, P. F., Birk, M., Boudon, V., Brown, L. R.,
650 Campargue, A., Champion, J. P., Chance, K., Coudert, L. H., Dana, V., Devi, V. M., Fally, S., Flaud, J. M.,
651 Gamache, R. R., Goldman, A., Jacquemart, D., Kleiner, I., Lacome, N., Lafferty, W. J., Mandin, J. Y., Massie, S. T.,

654 Mikhailenko, S. N., Miller, C. E., Moazzen-Ahmadi, N., Naumenko, O. V., Nikitin, A. V., Orphal, J., Perevalov, V.
655 I., Perrin, A., Predoi-Cross, A., Rinsland, C. P., Rotger, M., Šimečková, M., Smith, M. A. H., Sung, K., Tashkun, S.
656 A., Tennyson, J., Toth, R. A., Vandaele, A. C., and Vander Auwera, J.: The HITRAN 2008 molecular spectroscopic
657 database, *J. Quant. Spectrosc. Ra.*, 110, 533-572, <https://doi.org/10.1016/j.jqsrt.2009.02.013>, 2009.

658 Rothman, L. S., Jacquemart, D., Barbe, A., Chris Benner, D., Birk, M., Brown, L. R., Carleer, M. R., Chackerian Jr,
659 C., Chance, K., Coudert, L. H., Dana, V., Devi, V. M., Flaud, J. M., Gamache, R. R., Goldman, A., Hartmann, J. M.,
660 Jucks, K. W., Maki, A. G., Mandin, J. Y., Massie, S. T., Orphal, J., Perrin, A., Rinsland, C. P., Smith, M. A. H.,
661 Tennyson, J., Tolchenov, R. N., Toth, R. A., Vander Auwera, J., Varanasi, P., and Wagner, G.: The HITRAN 2004
662 molecular spectroscopic database, *J. Quant. Spectrosc. Ra.*, 96, 139-204, <https://doi.org/10.1016/j.jqsrt.2004.10.008>,
663 2005.

664 Smith, P., Bustamante, M., Ahammad, H., Clark, H., Dong, H., Elsiddig, E. A., Haberl, H., Harper, R., House, J.,
665 Jafari, M., Masera, O., Mbow, C., Ravindranath, N. H., Rice, C. W., Abad, C. R., Romanovskaya, A., Sperling, F.,
666 and Tubiello, F.: Agriculture, Forestry and Other Land Use (AFOLU). In: In: *Climate Change 2014: Mitigation of*
667 *Climate Change. Contribution of Working Group III to the Fifth Assessment Report of the Intergovernmental Panel*
668 *on Climate Change*, Edenhofer, O., Pichs-Madruga, R., Sokona, Y., Farahani, E., Kadner, S., Seyboth, K., Adler, A.,
669 Baum, I., Brunner, S., Eickemeier, P., Kriemann, B., Savolainen, J., Schlömer, S., von Stechow, C., Zwickel, T., and
670 Minx, J. C. (Eds.), Cambridge University Press, Cambridge, United Kingdom and New York, NY, USA, 2014.

671 Smith, T. E. L., Wooster, M. J., Tattaris, M., and Griffith, D. W. T.: Absolute accuracy and sensitivity analysis of
672 OP-FTIR retrievals of CO₂, CH₄ and CO over mole fractions representative of "clean air" and "polluted plumes",
673 *Atmos. Meas. Tech.*, 4, 97-116, <https://doi.org/10.5194/amt-4-97-2011>, 2011.

674 Tomkins, N. W., McGinn, S. M., Turner, D. A., and Charmley, E.: Comparison of open-circuit respiration chambers
675 with a micrometeorological method for determining methane emissions from beef cattle grazing a tropical pasture,
676 *Anim. Feed Sci. and Tech.*, 166-167, 240-247, <https://doi.org/10.1016/j.anifeedsci.2011.04.014>, 2011.

677 Tonini, M.: Measuring methane emissions from cattle using an open path FTIR tracer based method, Bachelor of
678 Science with Honours, Department of Chemistry, University of Wollongong, Wollongong, Australia, 68 pp., 2005.

679 VanderZaag, A. C., Flesch, T. K., Desjardins, R. L., Baldé, H., and Wright, T.: Measuring methane emissions from
680 two dairy farms: Seasonal and manure-management effects, *Agri. Forest Meteorol.*, 194, 259-267,
681 <https://doi.org/10.1016/j.agrformet.2014.02.003>, 2014.

682